EPRI | ELECTRIC POWER RESEARCH INSTITUTE

2020 TECHNICAL REPORT

# BWRVIP-332: BWR Vessel and Internals Project

## Testing and Evaluation of the Peach Bottom Unit 2 30° Surveillance Capsule

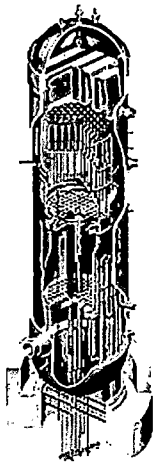

PREPARED UNDER THE NUCLEAR QA PROGRAM

# BWRVIP-332: BWR Vessel and Internals Project

## Testing and Evaluation of the Peach Bottom Unit 2 30° Surveillance Capsule

**3002018177**

Final Report, April 2020

EPRI Project Manager
R. Carter

All or a portion of the requirements of the EPRI Nuclear Quality Assurance Program apply to this product.

YES NO

ELECTRIC POWER RESEARCH INSTITUTE
3420 Hillview Avenue, Palo Alto, California 94304-1338 • PO Box 10412, Palo Alto, California 94303-0813 • USA
800.313.3774 • 650.855.2121 • askepri@epri.com • www.epri.com

## DISCLAIMER OF WARRANTIES AND LIMITATION OF LIABILITIES

THIS DOCUMENT WAS PREPARED BY THE ORGANIZATIONS NAMED BELOW AS AN ACCOUNT OF WORK SPONSORED OR COSPONSORED BY THE ELECTRIC POWER RESEARCH INSTITUTE, INC. (EPRI). NEITHER EPRI, ANY MEMBER OF EPRI, ANY COSPONSOR, THE ORGANIZATIONS BELOW, NOR ANY PERSON ACTING ON BEHALF OF ANY OF THEM:

(A) MAKES ANY WARRANTY OR REPRESENTATION WHATSOEVER, EXPRESS OR IMPLIED, (I) WITH RESPECT TO THE USE OF ANY INFORMATION, APPARATUS, METHOD, PROCESS, OR SIMILAR ITEM DISCLOSED IN THIS DOCUMENT, INCLUDING MERCHANTABILITY AND FITNESS FOR A PARTICULAR PURPOSE, OR (II) THAT SUCH USE DOES NOT INFRINGE ON OR INTERFERE WITH PRIVATELY OWNED RIGHTS, INCLUDING ANY PARTY'S INTELLECTUAL PROPERTY, OR (III) THAT THIS DOCUMENT IS SUITABLE TO ANY PARTICULAR USER'S CIRCUMSTANCE; OR

(B) ASSUMES RESPONSIBILITY FOR ANY DAMAGES OR OTHER LIABILITY WHATSOEVER (INCLUDING ANY CONSEQUENTIAL DAMAGES, EVEN IF EPRI OR ANY EPRI REPRESENTATIVE HAS BEEN ADVISED OF THE POSSIBILITY OF SUCH DAMAGES) RESULTING FROM YOUR SELECTION OR USE OF THIS DOCUMENT OR ANY INFORMATION, APPARATUS, METHOD, PROCESS, OR SIMILAR ITEM DISCLOSED IN THIS DOCUMENT.

REFERENCE HEREIN TO ANY SPECIFIC COMMERCIAL PRODUCT, PROCESS, OR SERVICE BY ITS TRADE NAME, TRADEMARK, MANUFACTURER, OR OTHERWISE, DOES NOT NECESSARILY CONSTITUTE OR IMPLY ITS ENDORSEMENT, RECOMMENDATION, OR FAVORING BY EPRI.

THE FOLLOWING ORGANIZATIONS PREPARED THIS REPORT:

**Electric Power Research Institute (EPRI)**

**MP Machinery & Testing, LLC**

**TransWare Enterprises Inc.**

THE TECHNICAL CONTENTS OF THIS PRODUCT WERE PREPARED IN ACCORDANCE WITH THE EPRI QUALITY PROGRAM MANUAL THAT FULFILLS THE REQUIREMENTS OF 10 CFR 50 APPENDIX B. THIS PRODUCT IS SUBJECT TO THE REQUIREMENTS OF 10 CFR PART 21. CERTIFICATION OF CONFORMANCE CAN BE OBTAINED FROM EPRI.

## NOTE

For further information about EPRI, call the EPRI Customer Assistance Center at 800.313.3774 or e-mail askepri@epri.com.

# ACKNOWLEDGMENTS

The following organizations prepared this report:

Electric Power Research Insitute (EPRI)
3420 Hillview Ave.
Palo Alto, CA 94304

Principal Investigators
E. Long
R. Carter

MP Machinery & Testing, LLC
2161 Sandy Drive
State College, PA 16803

Principal Investigator
Dr. M. P. Manahan, Sr.

TransWare Enterprises Inc.
1565 Mediterranean Drive
Sycamore, IL 60178

Principal Investigators
D. Jones
A. Scheppert
S. Wagstaff
K. Watkins

This report describes research sponsored by EPRI and its BWRVIP participating members.

This publication is a corporate document that should be cited in the literature in the following manner:

*BWRVIP-332: BWR Vessel and Internals Project—Testing and Evaluation of the Peach Bottom Unit 2 30° Surveillance Capsule.* EPRI, Palo Alto, CA: 2020. 3002018177.

# PRODUCT DESCRIPTION

In the late 1990s, a Boiling Water Reactor Vessel and Internals Project (BWRVIP) Integrated Surveillance Program (ISP) was developed to improve the surveillance of the U.S. BWR fleet. This report describes testing and evaluation of the Peach Bottom Unit 2 (PB2) Atomic Power Station 30° surveillance capsule. These results will be used to monitor embrittlement as part of the BWRVIP ISP.

## Background

The BWRVIP ISP represents a major enhancement to the process of monitoring embrittlement for the U.S. fleet of BWRs. The ISP optimizes surveillance capsule tests while at the same time maximizing the quantity and quality of data; thus, resulting in a more cost-effective program. The BWRVIP ISP provides more representative data that can be used to assess embrittlement in reactor pressure vessel (RPV) beltline materials and improve trend curves in the BWR range of irradiation conditions.

## Challenges and Objectives

Neutron irradiation exposure reduces the toughness of reactor vessel steel plates, welds, and forgings. The objectives of this project were twofold:

- To document the results of neutron dosimetry and Charpy V-notch toughness tests for the surveillance materials (plate heat C2761-2 and weld heat PB2 electroslag weld [ESW]) in the Peach Bottom Unit 2 30° surveillance capsule.
- To compare the results with the embrittlement trend prediction of the U.S. Nuclear Regulatory Commission (U.S. NRC) Regulatory Guide 1.99, Revision 2.

## Approach

The Peach Bottom Unit 2 30° surveillance capsule had been irradiated in the reactor since plant startup. The surveillance capsule contained flux wires for neutron flux monitoring, Charpy V-notch impact test specimens, and tensile specimens. The project team removed the capsule from the reactor in 2018 and transported it to facilities for testing and evaluation. The team used dosimetry to gather information about the neutron fluence accrual of specimens from the capsule. They then performed a neutron transport calculation in accordance with Regulatory Guide 1.190 and compared it to the results from the dosimetry. Testing of Charpy V-notch specimens was performed according to the American Society for Testing and Materials (ASTM) standards.

## Results and Findings

The report includes capsule neutron exposure and Charpy V-notch test results for Peach Bottom Unit 2 surveillance plate heat C2761-2 and surveillance weld heat PB2 ESW. The project compared irradiated Charpy data to unirradiated data in order to determine the shifts in Charpy index temperatures for the surveillance plate and weld materials due to irradiation. The measured shift for the surveillance plate and weld are less than the predicted shift + margin using

Regulatory Guide 1.99, Revision 2. Researchers also measured flux wires, determined a fluence value for the 30° surveillance capsule, and calculated a revised fluence value for the previously tested 120° surveillance capsule.

## Applications, Value, and Use

Results of this work will be used in the BWRVIP ISP that integrates individual BWR surveillance programs into a single program. The ISP provides data of high quality to monitor BWR vessel embrittlement. The ISP results in significant cost savings to the BWR fleet and provides more accurate monitoring of embrittlement in BWR vessels.


## Keywords

BWR
Charpy V-notch testing
Mechanical properties
Radiation embrittlement
Reactor pressure vessel integrity
Reactor vessel surveillance program

ELECTRIC POWER RESEARCH INSTITUTE

# EXECUTIVE SUMMARY

**Deliverable Number: 3002018177**

**Product Type: Technical Report**

## Product Title: BWRVIP-332: BWR Vessel and Internals Project—Testing and Evaluation of the Peach Bottom Unit 2 30° Surveillance Capsule

**PRIMARY AUDIENCE:** Plant engineers responsible for reactor vessel integrity

**SECONDARY AUDIENCE:** Boiling Water Reactor Vessel and Internals Project (BWRVIP) Program Owners

### KEY RESEARCH QUESTION

The objectives of this project were:

- To withdraw and test the Peach Bottom Unit 2 30° surveillance capsule per the approved test matrix of the BWRVIP Integrated Surveillance Program (ISP) (BWRVIP-86, Revision 1-A).
- To document the results of neutron dosimetry and Charpy V-notch toughness tests for the surveillance materials (plate heat C2761-2 and weld heat PB2 electroslag weld [ESW]) per American Society for Testing and Materials (ASTM) E 185-82, and determine capsule fluence per U.S. Nuclear Regulatory Commission (U.S. NRC) Regulatory Guide 1.190.
- To compare the results with embrittlement trend predictions of the U.S. NRC Regulatory Guide 1.99, Revision 2.

### RESEARCH OVERVIEW

The BWRVIP ISP combines individual BWR surveillance programs into a single program that monitors the reduction in toughness of reactor vessel steel plates, welds, and forgings as a result of neutron irradiation exposure. The Peach Bottom Unit 2 30° surveillance capsule was withdrawn and tested per the schedule in BWRVIP-86, Revision 1-A. The capsule had been irradiated in the reactor since plant startup, and contained flux wires for neutron flux monitoring, Charpy V-notch impact test specimens, and tensile specimens. The project team removed the capsule from the reactor in 2018 and transported it to facilities for testing and evaluation. The team used dosimetry to gather information about the neutron fluence accrual of the capsule specimens. They then performed a neutron transport calculation in accordance with Regulatory Guide 1.190 and compared it to the dosimetry results. Testing of Charpy V-notch specimens was performed according to ASTM standards.

### KEY FINDINGS

- The report includes capsule neutron exposure and Charpy V-notch test results for Peach Bottom Unit 2 surveillance plate heat C2761-2 and surveillance weld heat PB2 ESW.
- The project compared irradiated Charpy data to unirradiated data in order to determine the shifts in Charpy index temperatures for the surveillance plate and surveillance weld materials due to irradiation.
- For the surveillance plate, the measured shift is less than the predicted shift plus margin using Regulatory Guide 1.99, Revision 2. For the surveillance weld, the measured shift is less than the predicted shift plus margin using Regulatory Guide 1.99, Revision 2.
- Researchers measured flux wires, performed a fluence calculation to determine the fluence for the 30° surveillance capsule, and an updated fluence value for the previously tested 120° surveillance capsule.

EPRI | ELECTRIC POWER RESEARCH INSTITUTE

# EXECUTIVE SUMMARY

## WHY THIS MATTERS

Results of this work will be used in the BWRVIP ISP, which is utilized by U.S. BWR fleet owners to satisfy the requirements of 10 CFR 50 Appendix G and Appendix H. The ISP provides high quality data to monitor BWR vessel embrittlement. The ISP results in significant cost savings for the BWR fleet, and provides more accurate monitoring of embrittlement in BWR vessels. Plants for which the Peach Bottom Unit 2 surveillance materials are assigned as the representative surveillance materials under the ISP must consider these test results in development of vessel integrity evaluations and plant operating limit curves.

## HOW TO APPLY RESULTS

Instructions for use of ISP data are provided in the following technical report:

- *BWRVIP-135, Revision 3: BWR Vessel and Internals Project, Integrated Surveillance Program (ISP) Data Source Book and Plant Evaluations.* EPRI, Palo Alto, CA: 2014. 3002003144.

## LEARNING AND ENGAGEMENT OPPORTUNITIES

- The program plan for the BWRVIP ISP is described in the following technical report: *BWRVIP-86, Revision 1-A: BWR Vessel and Internals Project, Updated BWR Integrated Surveillance Program (ISP) Implementation Plan.* EPRI, Palo Alto, CA: 2012. 1025144.
- Data collected under the ISP and instructions for use of the data are contained in the following technical report: *BWRVIP-135, Revision 3: BWR Vessel and Internals Project, Integrated Surveillance Program (ISP) Data Source Book and Plant Evaluations*, EPRI, Palo Alto, CA: 2014. 3002003144.

**EPRI CONTACT:** Robert G. Carter, Technical Executive, bcarter@epri.com

**PROGRAM:** Boiling Water Reactor Vessel and Internals Program (BWRVIP), P41.01.03

**IMPLEMENTATION CATEGORY:** Category 1 - Regulatory



**Electric Power Research Institute**
3420 Hillview Avenue, Palo Alto, California 94304-1338 • PO Box 10412, Palo Alto, California 94303-0813 USA
800.313.3774 • 650.855.2121 • askepri@epri.com • www.epri.com

# CONTENTS

# LIST OF FIGURES

# LIST OF TABLES

# 1
# INTRODUCTION

Test coupons of reactor vessel ferritic beltline materials are irradiated in reactor surveillance capsules to facilitate evaluation of vessel fracture toughness in vessel integrity evaluations. The key values that characterize fracture toughness are the reference temperature of nil-ductility transition ($RT_{NDT}$) and the upper shelf energy (USE). These are defined in 10CFR50, Appendix G [1] and in Appendix G of the ASME Boiler and Pressure Vessel Code, Section XI [2]. Appendix H of 10CFR50 [1] and ASTM E185-82 [3] establish the methods to be used for testing of surveillance capsule materials.

In the late 1990s, the BWR Vessel and Internals Project (BWRVIP) initiated the BWRVIP Integrated Surveillance Program (ISP) [4], and the BWRVIP assumed responsibility for testing and evaluation of ISP capsules. The surveillance plate and weld from the Peach Bottom Unit 2 (PB2) Nuclear Station (hereinafter, Peach Bottom Unit 2) were designated as "ISP representative surveillance materials" to be tested by the ISP according to an approved capsule withdrawal and test schedule.

This report addresses the withdrawal and testing of the Peach Bottom Unit 2 30° surveillance capsule. The capsule contained flux wires for neutron flux monitoring, Charpy V-notch impact test specimens, and tensile specimens. The capsule was irradiated for 22 cycles of operation before it was removed in October 2018 and shipped to MP Machinery & Testing, LLC for opening and testing of the Charpy V-notch surveillance specimens. Evaluation of the fluence environment was conducted by TransWare Enterprises, Inc. Final evaluation of the Charpy test data and irradiated material properties and compilation of this report were performed by EPRI. The Charpy V-notch surveillance materials were tested per ASTM E185-82, and the information and the associated evaluations provided in this report have been performed in accordance with the requirements of 10CFR50, Appendix B [5].

This report compares the irradiated material properties of surveillance plate heat C2761-2 and surveillance weld heat PB2 ESW to their unirradiated (e.g., baseline) properties. The observed embrittlement (as characterized by the shift in the Charpy energy curve 30 ft-lb (41J) index temperature or $\Delta T_{30}$) is compared to that predicted by U.S. Nuclear Regulatory Commission (U.S. NRC) Regulatory Guide 1.99, Revision 2 [6]. Other BWRVIP ISP reports will integrate the results from the 30° surveillance capsule with the results from the Peach Bottom Unit 2 120° surveillance capsule (withdrawn in 1987) for a broader characterization of embrittlement behavior.

## 1.1 Implementation Requirements

The results documented in this report will be utilized by the BWRVIP ISP and by individual utilities to demonstrate compliance with 10CFR50, Appendix H, Reactor Vessel Material Surveillance Program Requirements. Therefore, the implementation requirements of 10CFR50, Appendix H govern and the implementation requirements of Nuclear Energy Institute (NEI) 03-08, Guideline for the Management of Materials Issues [7], are not applicable.

# 2
# MATERIALS AND TEST SPECIMEN DESCRIPTION

The General Electric (GE) designed Peach Bottom Unit 2 30° surveillance capsule was removed from the plant and shipped to MP Machinery and Testing, LLC (MPM) for analysis. The capsule contained a total of three Charpy packets and four tensile tubes. The 30° surveillance capsule is an original plant capsule and has been irradiated in the plant since initial startup. This is the second surveillance capsule to be removed from Peach Bottom Unit 2 and tested. The 120° surveillance capsule was tested by GE and the results are reported in Reference [8].

## 2.1 Dosimeters

The dosimetry wires were located along the ends of the Charpy specimens within the Charpy packets during irradiation. Each of the three Charpy packets contained one high purity iron wire, one high purity copper wire, and one high purity nickel wire for fluence evaluation. Further details on the exact wire locations during the irradiation are provided in the capsule opening discussion given in Section 2.3. A detailed discussion of the radiometric analysis of the capsule dosimetry wires is provided in Appendix A.

## 2.2 Test Materials

The Peach Bottom Unit 2 30° surveillance capsule Charpy V-notch specimen inventory, material descriptions, unirradiated (baseline) Charpy impact data, and previously measured data are summarized in this section of the report.

### *2.2.1 Capsule Loading Inventory*

The Peach Bottom Unit 2 30° surveillance capsule inventory is provided in Table 2-1. All of the capsule specimens, which include Charpy specimens, tensile specimens, and dosimeters, were recovered from the capsule basket. Testing was performed on all of the 36 Charpy specimens, and the dosimetry wires were counted and weighed to determine specific activities. All eight of the tensile specimens (three base, two weld, and three HAZ) remain untested and are being held in reserve for future surveillance program use. The technical advantage of storing the tensile specimens untested is that there will be options in the future for how these specimens will be used to obtain useful data. For example, the tensile specimen geometry is conducive to fabrication of sub-size Charpy as well as miniaturized Charpy V-notch specimens. Further, research is currently underway to develop testing methods which will enable the determination of plane-strain fracture toughness data from Charpy-sized specimens. With these new technologies in view, there may also be a need in the future for static and/or dynamic tensile data for use in the calculation of fracture toughness from experimental data obtained from Charpy specimens. Therefore, all of the tensile specimens have been placed into the archive storage so

that they can be tested when necessary in the future. The broken Charpy specimen halves have been added to long-term archive storage for future use in mechanical behavior specimen testing, chemistry analysis, and microstructural studies.

As indicated in Table 2-1, there were three Charpy packets in the capsule, and each contained three dosimetry wires (one Fe wire, one Cu wire, and one Ni wire) and 12 Charpy specimens. A drawing of the Charpy test specimen is shown in Figure 2-1 for reference. Photographs of the capsule are given in Figures 2-2 through 2-4. The markings on the outside of the capsule, including the reactor code and the capsule code, were recorded and verified.

**Table 2-1**
**Peach Bottom Unit 2 30° Surveillance Capsule Specimen Inventory**

| Charpy[1] Packet No.[2] | Number of Charpy Specimens | | | Number of Flux Wires | | | Relative Vertical Position |
|---|---|---|---|---|---|---|---|
| | Base | Weld | HAZ | Fe | Cu | Ni | |
| G1 | 12 | 0 | 0 | 1 | 1 | 1 | Lowest Charpy Packet in Basket |
| G2 | 0 | 12 | 0 | 1 | 1 | 1 | Middle Charpy Packet in Basket |
| G3 | 0 | 0 | 12 | 1 | 1 | 1 | Highest Charpy Packet in Basket |

1. The surveillance program also includes tensile specimens, but the tensile specimens were not tested. Four of the tensile specimens for this capsule were located at axial positions below Charpy packet G2 and above Charpy Packet G1. The other four tensile specimens for this capsule were located below Charpy packet G1.
2. The packet numbers in this table are organized by axial position in the capsule with packet G1 at the lowest elevation in the reactor and packet G3 at the highest elevation in the reactor.

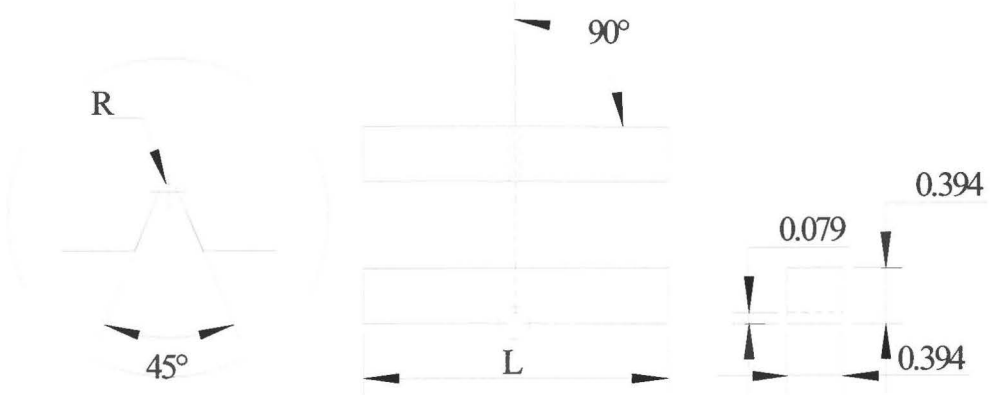


ASTM E23 [9] permissible variations shall be as follows:

| | |
|---|---|
| Notch length to edge: | 90 ± 2 degrees |
| Adjacent sides shall be at: | 90 degrees ± 10 minutes |
| Cross-sectional dimensions: | ± 0.003 inches |
| Length of specimen (L): | 2.165 (+0.0, -0.100) inches |
| Charpy Height (H) | 0.394 inches |
| Charpy Notch Depth | 0.079 inches |
| Centering of notch (L/2): | ± 0.039 inches |
| Angle of notch: | ± 1 degree |
| Radius of notch: | 0.010 ± 0.001 inches |
| Notch depth: | ± 0.001 inches |
| Finish requirements: | 63 μ-inch on notched surface and opposite face; 4 μ-inch elsewhere |

**Figure 2-1**
**Drawing Showing the Charpy Test Specimen Geometry and ASTM E23 [9] Permissible Variations**

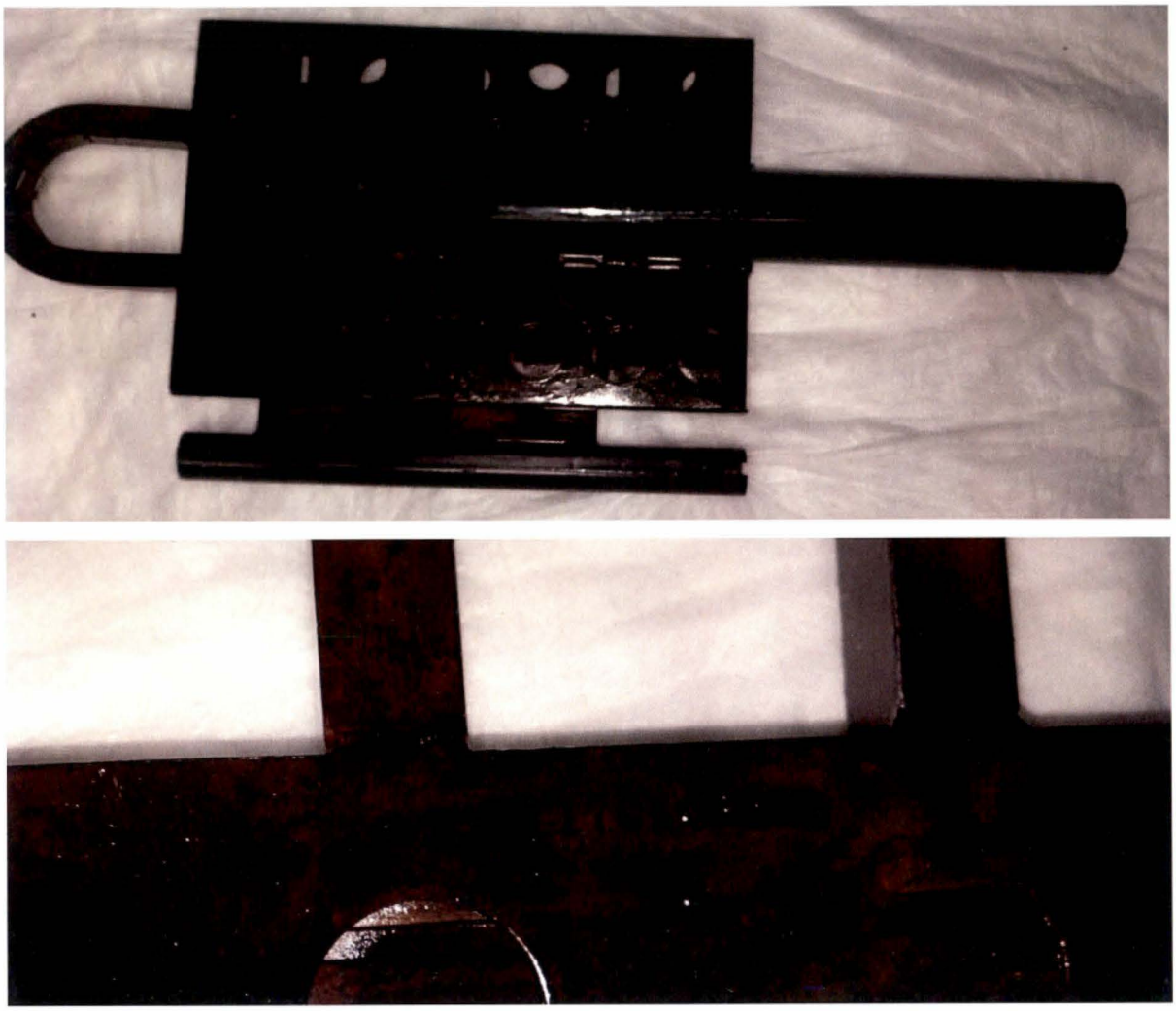

**Figure 2-2**
**Photograph of the Peach Bottom Unit 2 30° Capsule (top) and a Magnified View of the External Identification Markings (bottom)**

Figure 2-2 shows the side of the surveillance capsule which faced the reactor vessel. The identification code, "117C404BG1", was engraved near the hook.

**Figure 2-3**
**Photograph of the Peach Bottom Unit 2 30° Capsule (top) and a Magnified View of the Reactor and Capsule Codes Seen Near the Hook (bottom)**

Figure 2-3 shows the side of the surveillance capsule which faced the reactor core.

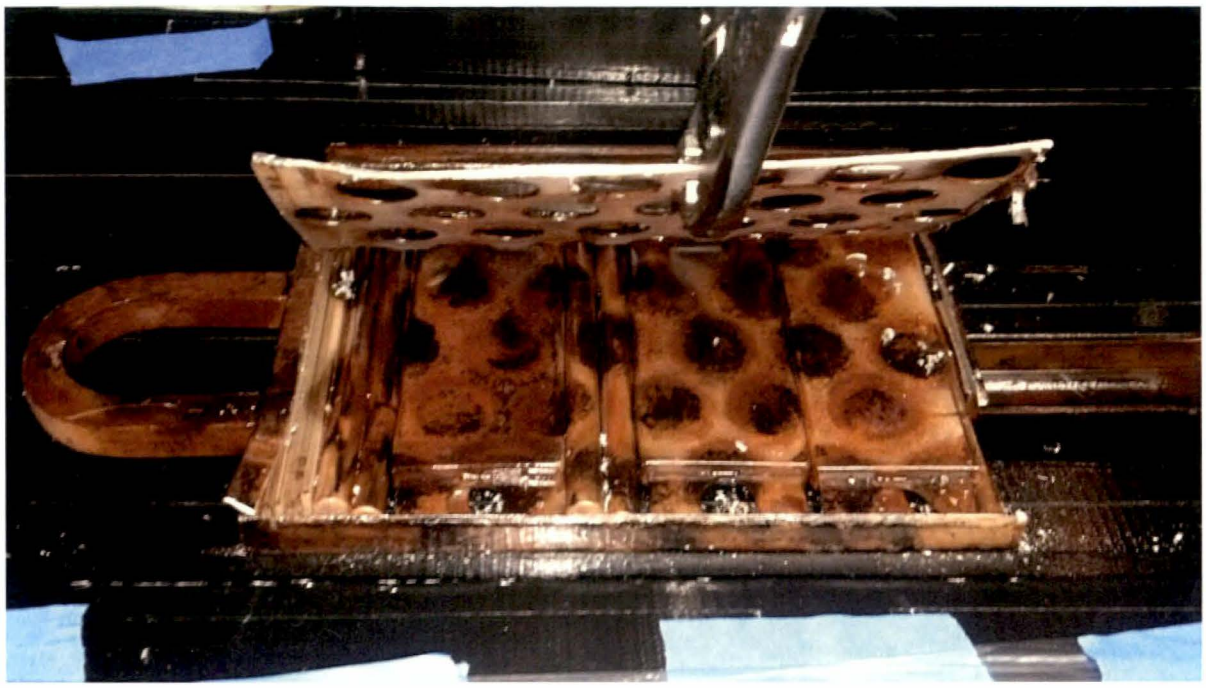

**Figure 2-4**
**Photograph of the Inside of the Peach Bottom Unit 2 30° Capsule**

### *2.2.2 Material Description*

The Peach Bottom Unit 2 surveillance program is described in a report issued by General Electric in Reference [8]. The Peach Bottom Unit 2 reactor pressure vessel (RPV) is a 251-inch diameter BWR/4 design. The pressure vessel construction was started by Babcock & Wilcox to the Winter 1965 addenda of the 1965 edition of the ASME Code. It was completed by Chicago Bridge & Iron, generally to the 1968 edition of the ASME Code. The pressure vessel shell and head plate materials are ASME SA302, Grade B low alloy steel, modified per Code Case 1339. The nozzles and closure flanges are ASTM A508 Class 2 low alloy steel, modified per Code Case 1332-2, and the closure flange bolting materials are ASTM A540 Grade B24 low alloy steel, modified by Code Cases 1335-2 and -4. The fabrication process employed double quench and temper heat treatment immediately after hot forming, then electroslag or submerged arc welding and post-weld heat treatment. The post-weld heat treatment was typically 30 hours at 1125 °F +/-25 °F.

The surveillance base metal specimens were machined from plate (Heat C2761-2) from the beltline. The test plate experienced heat treatment comparable to that of the beltline plates. Specimens were machined from the ¼ T and ¾ T positions in the plate, in the longitudinal orientation. The weld material and HAZ Charpy specimens were fabricated from trim-off pieces of plates from the beltline region (Heats C2761-2 and C2761-1) that were welded together by electroslag welding. All specimens are stamped on the sides or ends with the fabrication code listed on the Peach Bottom Unit 2 drawings.

### 2.2.3 Chemical Composition

Table 2-2 details the best estimate average chemistry values for plate heat C2761-2 surveillance material. Table 2-3 details the best estimate average chemistry values for weld heat PB2 ESW surveillance material. Chemical compositions are presented in weight percent. If there are multiple measurements on a single specimen, those are first averaged to yield a single value for that specimen, and then the different specimens are averaged to determine the heat best estimate.

**Table 2-2**
**Best Estimate Chemistry of Available Data Sets for Plate Heat C2761-2**

| Cu (wt%) | Ni (wt%) | P (wt%) | S (wt%) | Si (wt%) | Specimen ID | Source |
|---|---|---|---|---|---|---|
| 0.10 | 0.54 | 0.009 | — | — | 7K1 | Reference 8 |
| 0.10 | 0.53 | 0.011 | — | — | 7J5 | |
| 0.11 | 0.54 | 0.011 | 0.015 | 0.23 | Plate CMTR | |
| 0.10 | 0.54 | 0.010 | 0.015 | 0.23 | ←Best Estimate Average | |

**Table 2-3**
**Best Estimate Chemistry of Available Data Sets for Weld Heat PB2 ESW**

| Cu (wt%) | Ni (wt%) | P (wt%) | S (wt%) | Si (wt%) | Specimen ID | Source |
|---|---|---|---|---|---|---|
| 0.09 | 0.32 | 0.010 | — | — | Tensile 7KK | Reference 8 |
| 0.1 | 0.32 | 0.012 | — | — | Tensile 7KL | |
| 0.10 | 0.32 | 0.011 | — | — | ←Best Estimate Average | |

### 2.2.4 CVN Baseline Properties

Table 2-4 contains the unirradiated Charpy data for the C2761-2 surveillance plate material. Table 2-5 contains the unirradiated Charpy data for the PB2 ESW surveillance weld material.

**Table 2-4**
**Unirradiated Longitudinal Charpy V-Notch Impact Test Results for Surveillance Base Metal (Heat C2761-2) Specimens from the Peach Bottom Unit 2 Surveillance Program [8]**

| Base Unirradiated: Heat C2761-2, Longitudinal | | | | | | | |
|---|---|---|---|---|---|---|---|
| Specimen ID | Test Temperature | | Impact Energy | | Lateral Expansion | | Percent Shear |
| | °F | (°C) | ft-lb | (J) | mils | (mm) | % |
| 75K | -40 | (-40.0) | 18.5 | (25.08) | 14.5 | (0.37) | 0 |
| 763 | -20 | (-28.9) | 20.0 | (27.12) | 17.0 | (0.43) | 15 |
| 764 | 0 | (-17.8) | 30.0 | (40.67) | 28.0 | (0.71) | 20 |
| 76C | 20 | (-6.7) | 58.0 | (78.64) | 44.0 | (1.12) | 36 |
| 766 | 20 | (-6.7) | 68.0 | (92.20) | 49.0 | (1.24) | 33 |
| 75T | 40 | (4.4) | 77.0 | (104.40) | 58.0 | (1.47) | 40 |
| 75L | 60 | (15.6) | 100.0 | (135.58) | 70.5 | (1.79) | 60 |
| 76A | 80 | (26.7) | 112.0 | (151.85) | 79.0 | (2.01) | 82 |
| 75Y | 120 | (48.9) | 117.0 | (158.63) | 82.5 | (2.10) | 89 |
| 76B | 160 | (71.1) | 123.5 | (167.44) | 88.5 | (2.25) | 100 |
| 762 | 200 | (93.3) | 123.5 | (167.44) | 84.5 | (2.15) | 100 |
| 76D | 300 | (148.9) | 134.5 | (182.36) | 84.5 | (2.15) | 100 |

**Table 2-5**
**Unirradiated Charpy V-Notch Impact Test Results for Surveillance Weld Metal (Heat PB2 ESW) Specimens from the Peach Bottom Unit 2 Surveillance Program [8]**

| Weld Unirradiated: Heat PB2 ESW | | | | | | | |
|---|---|---|---|---|---|---|---|
| Specimen ID | Test Temperature | | Impact Energy | | Lateral Expansion | | Percent Shear |
| | °F | (°C) | ft-lb | (J) | mils | (mm) | % |
| 7AE | -40 | (-40.0) | 17.5 | (23.73) | 14 | (0.36) | 0 |
| 7BB | -20 | (-28.9) | 20 | (27.12) | 19 | (0.48) | 6 |
| 7BC | 0 | (-17.8) | 32 | (43.39) | 27 | (0.69) | 8 |
| 7BK | 20 | (-6.7) | 38 | (51.52) | 28.5 | (0.72) | 10 |
| 7B1 | 40 | (4.4) | 35.5 | (48.13) | 40 | (1.02) | 15 |
| 7AU | 60 | (15.6) | 73.5 | (99.65) | 57 | (1.45) | 37 |
| 7C6 | 60 | (15.6) | 63 | (85.42) | 50 | (1.27) | 38 |
| 7BP | 80 | (26.7) | 68 | (92.20) | 53.5 | (1.36) | 53 |
| 7B2 | 120 | (48.9) | 91 | (123.38) | 67 | (1.70) | 77 |
| 7BU | 160 | (71.1) | 100.5 | (136.26) | 80 | (2.03) | 88 |
| 7B7 | 200 | (93.3) | 106 | (143.72) | 81.5 | (2.07) | 100 |
| 7CE | 300 | (148.9) | 111 | (150.50) | 76 | (1.93) | 100 |

The baseline test data were fit to a hyperbolic tangent curve using the computer program CVGRAPH [10]. Figures 2-5 and 2-6 show the fitted Charpy energy data curve for the unirradiated plate and weld, respectively. Figures 2-7 and 2-8 show the fitted lateral expansion curve for the unirradiated plate and weld, respectively. Table 2-6 summarizes the unirradiated (baseline) Charpy V-notch properties (index temperatures) of plate heat C2761-2 and weld heat PB2 ESW. In this table and throughout this report, $T_{30}$ is the 30 ft-lb (41 J) transition temperature; $T_{50}$ is the 50 ft-lb (68 J) transition temperature; $T_{35mil}$ is the 35 mil (0.89 mm) lateral expansion temperature; and USE is the average energy absorption at full shear fracture appearance.

**Table 2-6**
**Baseline CVN Properties**

| Material Identity | Material | $T_{30}$ °F (°C) | $T_{50}$ °F (°C) | $T_{35mil}$ °F (°C) | Upper Shelf Energy (USE) ft-lb (J) |
|---|---|---|---|---|---|
| C2761-2 (LT Orientation) | Peach Bottom Unit 2 Surveillance Plate | -9.6 (-23.1) | 12.3 (-10.9) | 6.4 (-14.2) | 127.2 (172.5) |
| PB2 ESW | Peach Bottom Unit 2 Surveillance Weld | 3.0 (-16.1) | 41.4 (5.2) | 25.1 (-3.8) | 110.9 (150.4) |

## Plate Heat C2761-2 (PB2)

CVGraph 6.02: Hyperbolic Tangent Curve Printed on 3/24/2020 6:47 AM

**A = 64.85 B = 62.35 C = 56.27 T0 = 25.87 D = 0.00**

Correlation Coefficient = 0.992

Equation is A + B * [Tanh((T-T0)/(C+DT))]

Upper Shelf Energy = 127.20 (Fixed) Lower Shelf Energy = 2.50 (Fixed)

Temp@30 ft-lbs= -9.60° F Temp@35 ft-lbs= -3.40° F Temp@50 ft-lbs= 12.30° F

Plant: **Peach Bottom 2** Material: **SA302BM** Heat: **C2761-2**
Orientation: **LT** Capsule: **UNIRRA** Fluence: **0.00E+000 n/cm²**

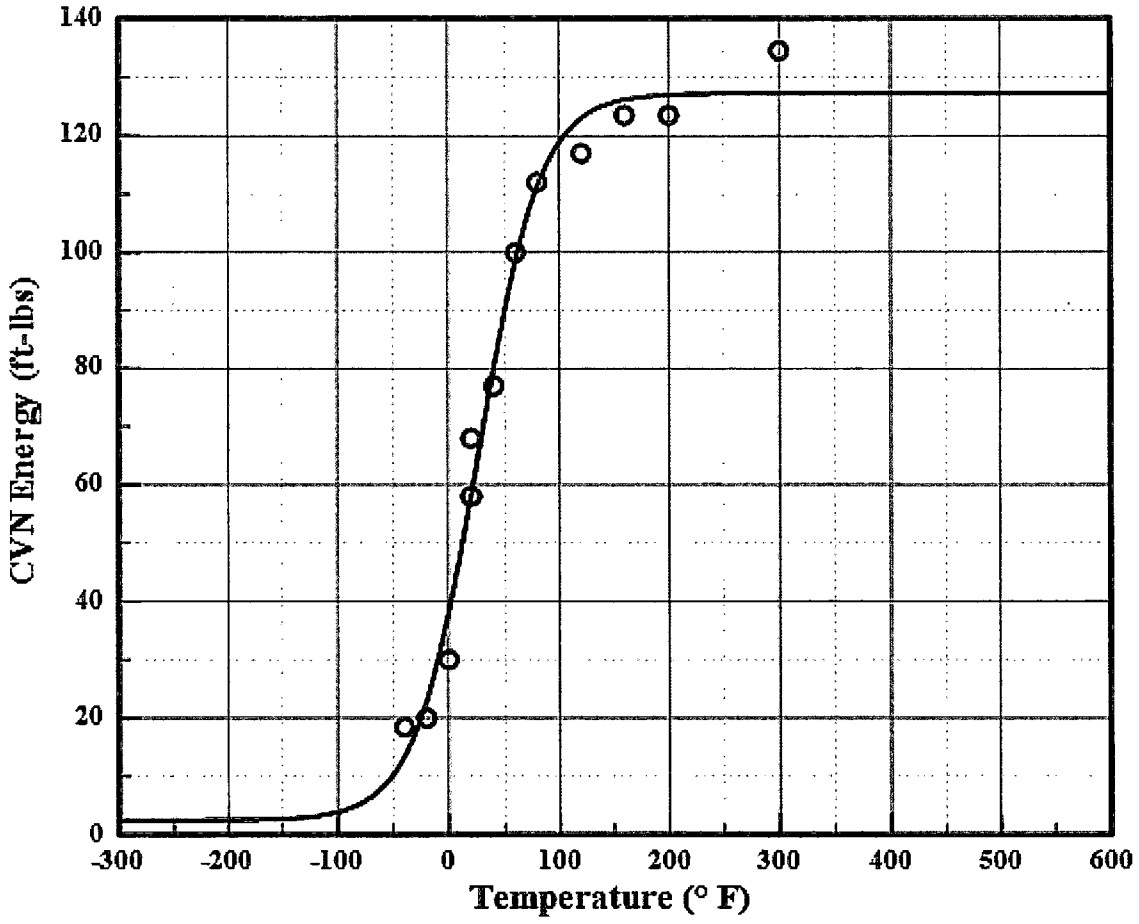


CVGraph 6.02 03/24/2020 Page 1/2

**Figure 2-5**
**Charpy Energy Plot for Plate Heat C2761-2 (LT) Unirradiated**

Plant: **Peach Bottom 2** Material: **SA302BM** Heat: **C2761-2**
Orientation: **LT** Capsule: **UNIRRA** Fluence: **0.00E+000 n/cm²**

# Plate Heat C2761-2 (PB2)

# Charpy V-Notch Data

| Temperature (° F) | Input CVN | Computed CVN | Differential |
|---|---|---|---|
| -40 | 18.5 | 13.4 | 5.06 |
| -20 | 20.0 | 22.9 | -2.92 |
| 0 | 30.0 | 38.0 | -8.05 |
| 20 | 58.0 | 58.4 | -0.37 |
| 20 | 68.0 | 58.4 | 9.63 |
| 40 | 77.0 | 80.2 | -3.19 |
| 60 | 100.0 | 98.6 | 1.37 |
| 80 | 112.0 | 111.3 | 0.69 |
| 120 | 117.0 | 123.0 | -5.96 |
| 160 | 123.5 | 126.1 | -2.65 |
| 200 | 123.5 | 126.9 | -3.44 |
| 300 | 134.5 | 127.2 | 7.31 |

CVGraph 6.02 03/24/2020 Page 2/2

**Figure 2-5 (continued)**
**Charpy Energy Plot for Plate Heat C2761-2 (LT) Unirradiated**

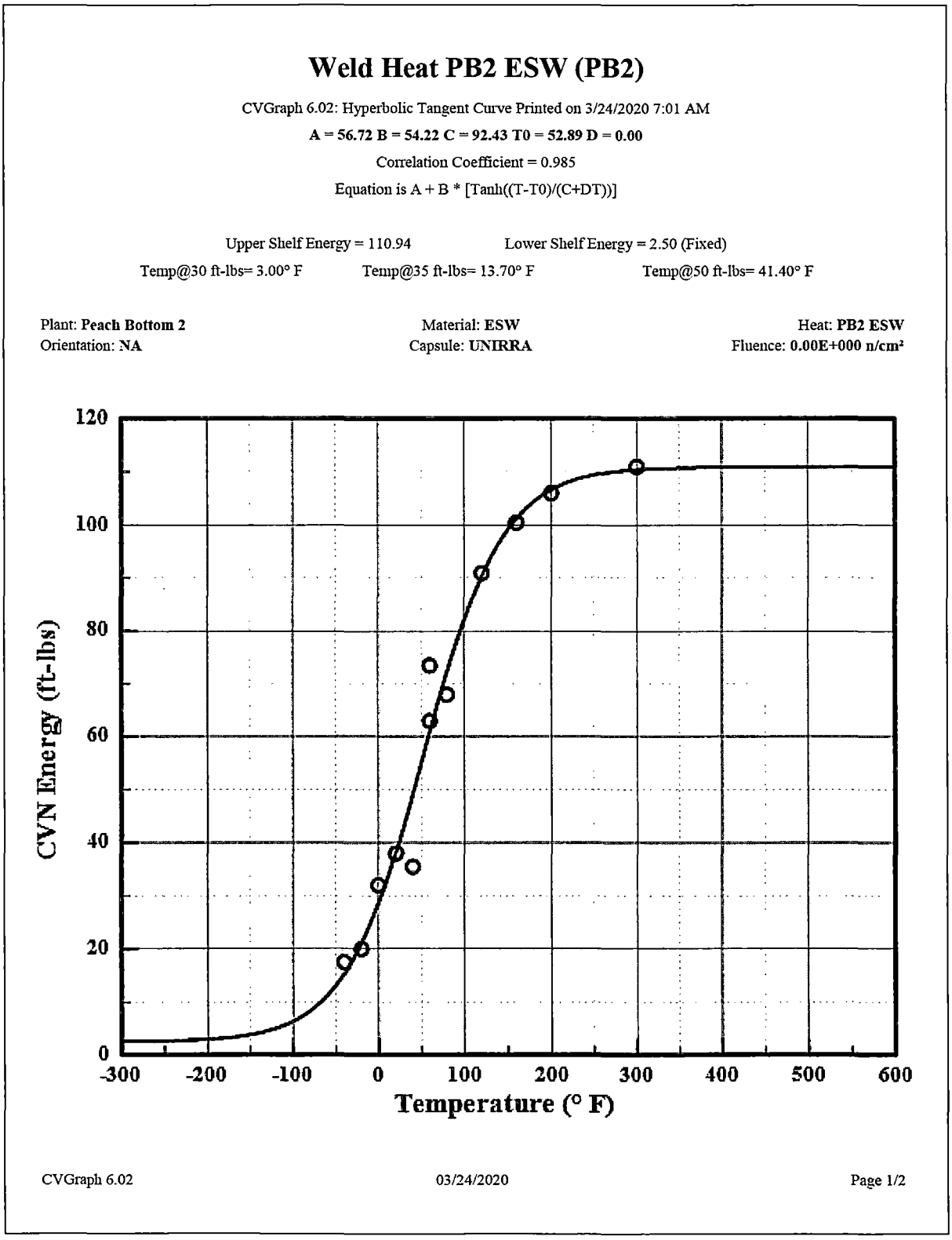


**Figure 2-6**
**Charpy Energy Plot for Weld Heat PB2 ESW Unirradiated**

Plant: **Peach Bottom 2** Material: **ESW** Heat: **PB2 ESW**
Orientation: **NA** Capsule: **UNIRRA** Fluence: **0.00E+000 n/cm²**

# Weld Heat PB2 ESW (PB2)

## Charpy V-Notch Data

| Temperature (° F) | Input CVN | Computed CVN | Differential |
|---|---|---|---|
| -40 | 17.5 | 15.3 | 2.19 |
| -20 | 20.0 | 21.1 | -1.06 |
| 0 | 32.0 | 28.7 | 3.31 |
| 20 | 38.0 | 38.2 | -0.20 |
| 40 | 35.5 | 49.2 | -13.71 |
| 60 | 73.5 | 60.9 | 12.62 |
| 60 | 63.0 | 60.9 | 2.12 |
| 80 | 68.0 | 72.2 | -4.18 |
| 120 | 91.0 | 90.4 | 0.63 |
| 160 | 100.5 | 101.2 | -0.71 |
| 200 | 106.0 | 106.6 | -0.62 |
| 300 | 111.0 | 110.4 | 0.58 |

CVGraph 6.02 03/24/2020 Page 2/2

**Figure 2-6 (continued)**
**Charpy Energy Plot for Weld Heat PB2 ESW Unirradiated**

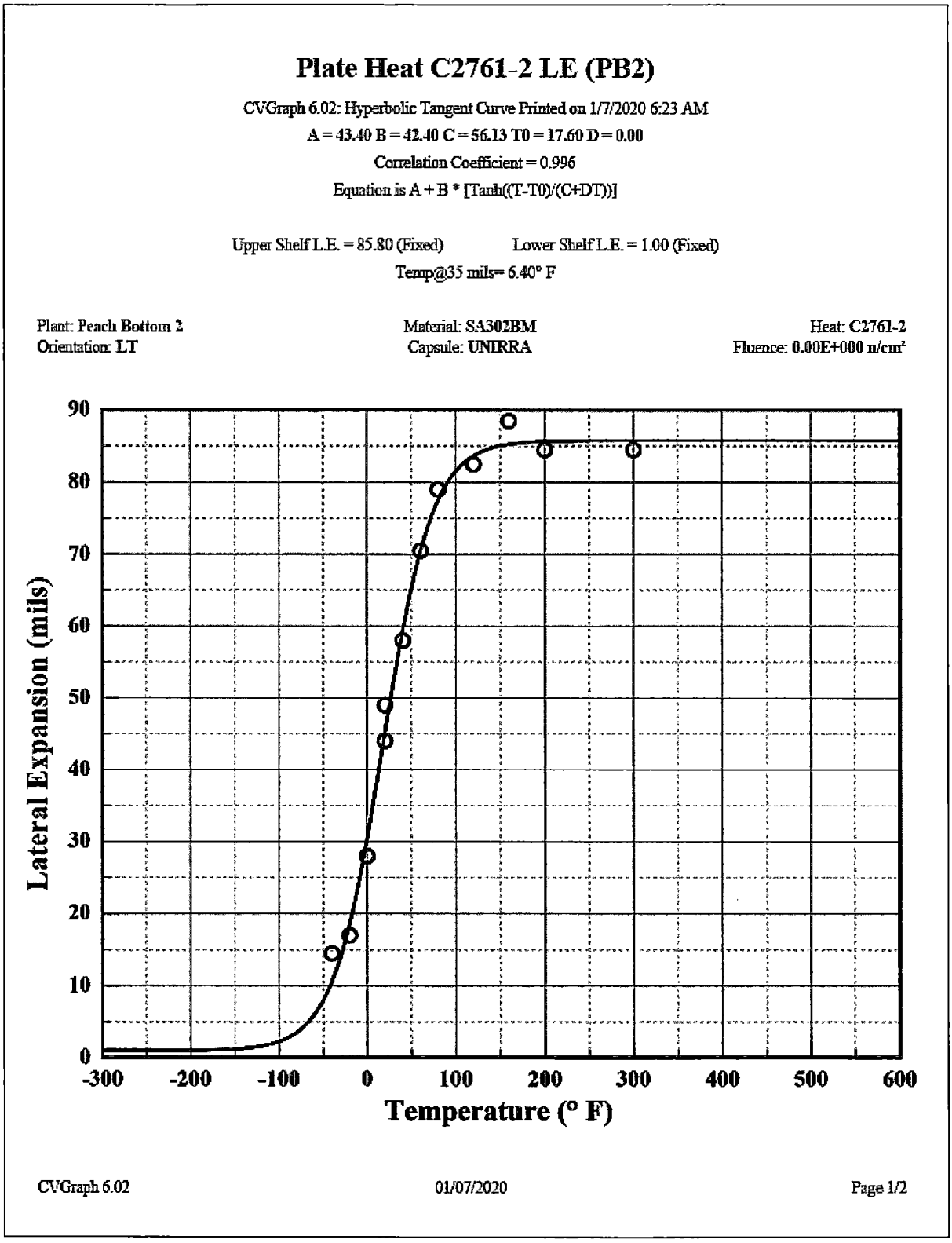


**Figure 2-7**
**Lateral Expansion Plot for Plate Heat C2761-2 (LT) Unirradiated**

Plant: **Peach Bottom 2**
Orientation: **LT**

Material: **SA302BM**
Capsule: **UNIRRA**

Heat: **C2761-2**
Fluence: **0.00E+000 n/cm²**

## Plate Heat C2761-2 LE (PB2)

## Charpy V-Notch Data

| Temperature (° F) | Input L. E. | Computed L. E. | Differential |
|---|---|---|---|
| -40 | 14.5 | 10.7 | 3.85 |
| -20 | 17.0 | 18.6 | -1.60 |
| 0 | 28.0 | 30.5 | -2.53 |
| 20 | 44.0 | 45.2 | -1.22 |
| 20 | 49.0 | 45.2 | 3.78 |
| 40 | 58.0 | 59.5 | -1.48 |
| 60 | 70.5 | 70.5 | 0.03 |
| 80 | 79.0 | 77.5 | 1.48 |
| 120 | 82.5 | 83.6 | -1.15 |
| 160 | 88.5 | 85.3 | 3.23 |
| 200 | 84.5 | 85.7 | -1.17 |
| 300 | 84.5 | 85.8 | -1.30 |

CVGraph 6.02 01/07/2020 Page 2/2

**Figure 2-7 (continued)**
**Lateral Expansion Plot for Plate Heat C2761-2 (LT) Unirradiated**

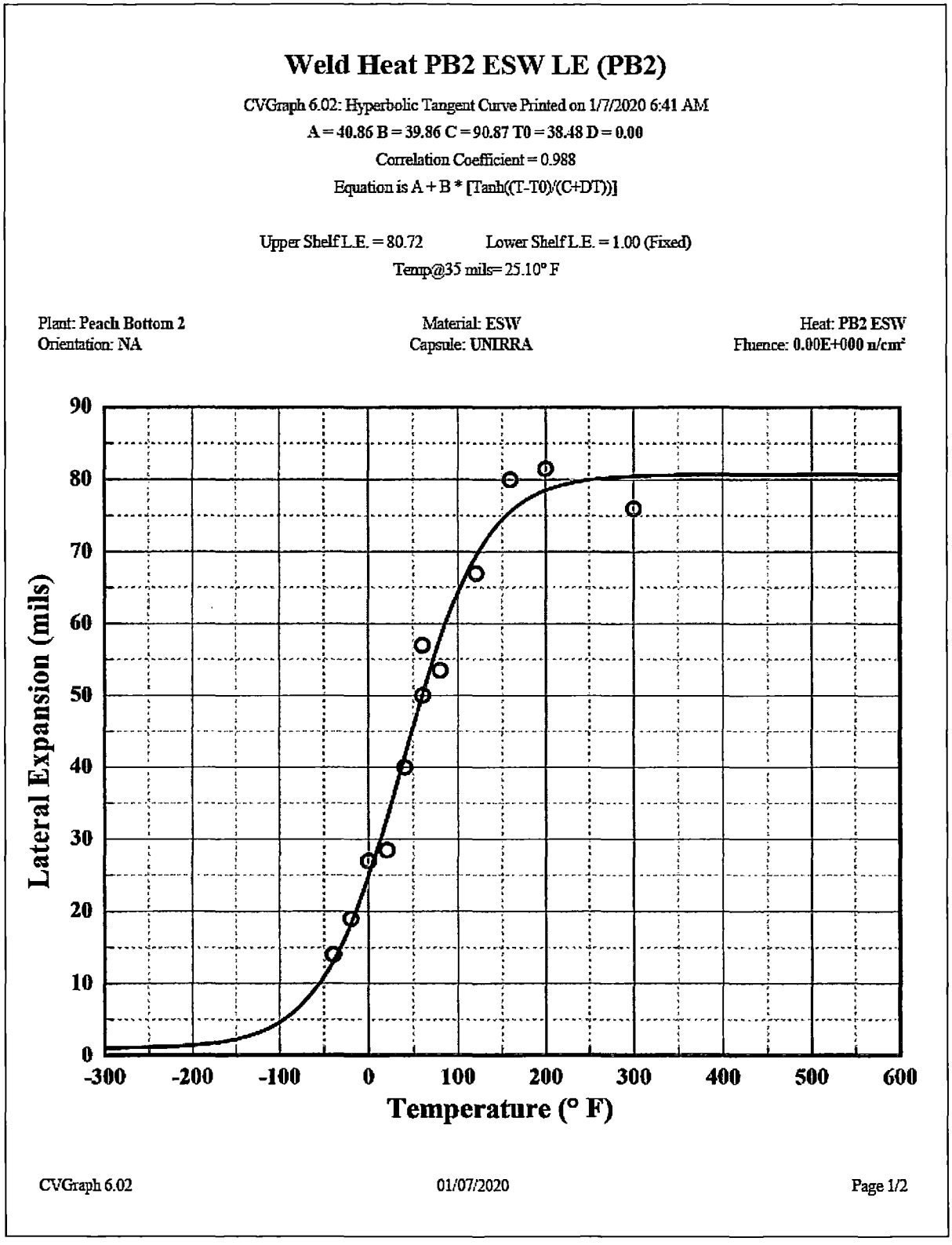


**Figure 2-8**
**Lateral Expansion Plot for Weld Heat PB2 ESW Unirradiated**

Plant: Peach Bottom 2 | Material: ESW | Heat: PB2 ESW
Orientation: NA | Capsule: UNIRRA | Fluence: 0.00E+000 n/cm²

## Weld Heat PB2 ESW LE (PB2)

## Charpy V-Notch Data

| Temperature (° F) | Input L. E. | Computed L. E. | Differential |
|---|---|---|---|
| -40 | 14.0 | 13.0 | 0.97 |
| -20 | 19.0 | 18.2 | 0.75 |
| 0 | 27.0 | 24.9 | 2.08 |
| 20 | 28.5 | 32.9 | -4.36 |
| 40 | 40.0 | 41.5 | -1.53 |
| 60 | 57.0 | 50.1 | 6.87 |
| 60 | 50.0 | 50.1 | -0.13 |
| 80 | 53.5 | 57.9 | -4.40 |
| 120 | 67.0 | 69.4 | -2.36 |
| 160 | 80.0 | 75.6 | 4.42 |
| 200 | 81.5 | 78.5 | 3.00 |
| 300 | 76.0 | 80.5 | -4.47 |

CVGraph 6.02 | 01/07/2020 | Page 2/2

**Figure 2-8 (continued)**
**Lateral Expansion Plot for Weld Heat PB2 ESW Unirradiated**

## 2.3 Capsule Opening

As shown in Figures 2-2 through 2-4, the 30° capsule consisted of a container holding three Charpy packets and four tensile tubes. Each Charpy packet contained 12 Charpy specimens. The outside of the capsule had identification markings which could be clearly read. On one side, the capsule container was marked with the reactor and capsule codes. The reactor code matches the reactor code in Reference [8]. The capsule container was engraved with the marking "117C404BG1" on the side facing the core.

Attention was paid to the location of the Charpy packets, specimens and dosimetry wires during disassembly of the capsule. The dosimetry wire locations along the ends of the Charpy specimens are shown in Figure 2-9. Referring to the figure, the 12 base metal specimens in the G1 Charpy packet were installed at the bottom of the capsule, the 12 weld metal specimens in the G2 Charpy packet were installed near the middle of the capsule, and the 12 HAZ specimens in the G3 Charpy packet were installed in the top of the capsule. Specimen orientation can be seen in Figure 2-9 and the inside of the packets is shown in Figures 2-10 through 2-12. The dosimetry wires and Charpy specimens were placed in individually marked containers for positive identification throughout the work.

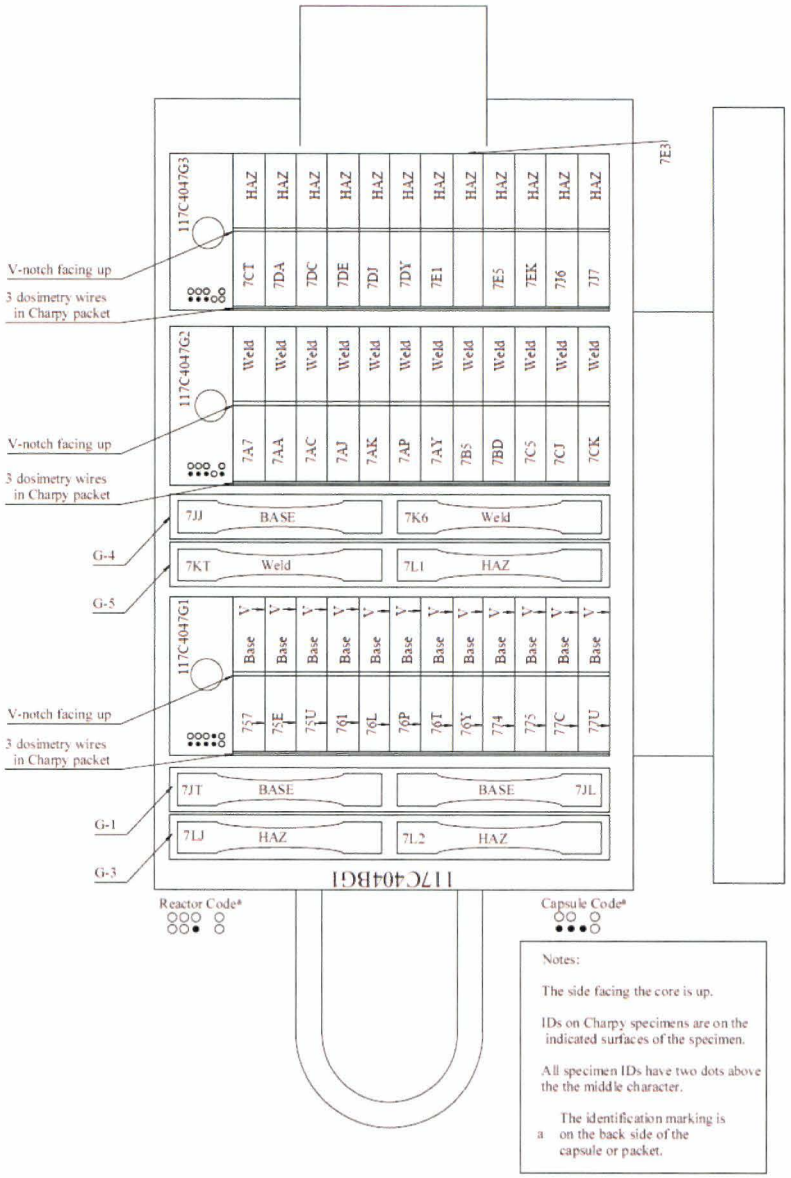


**Figure 2-9**
**Drawing of the Identification Markings Found Inside the Peach Bottom Unit 2 30° Capsule**

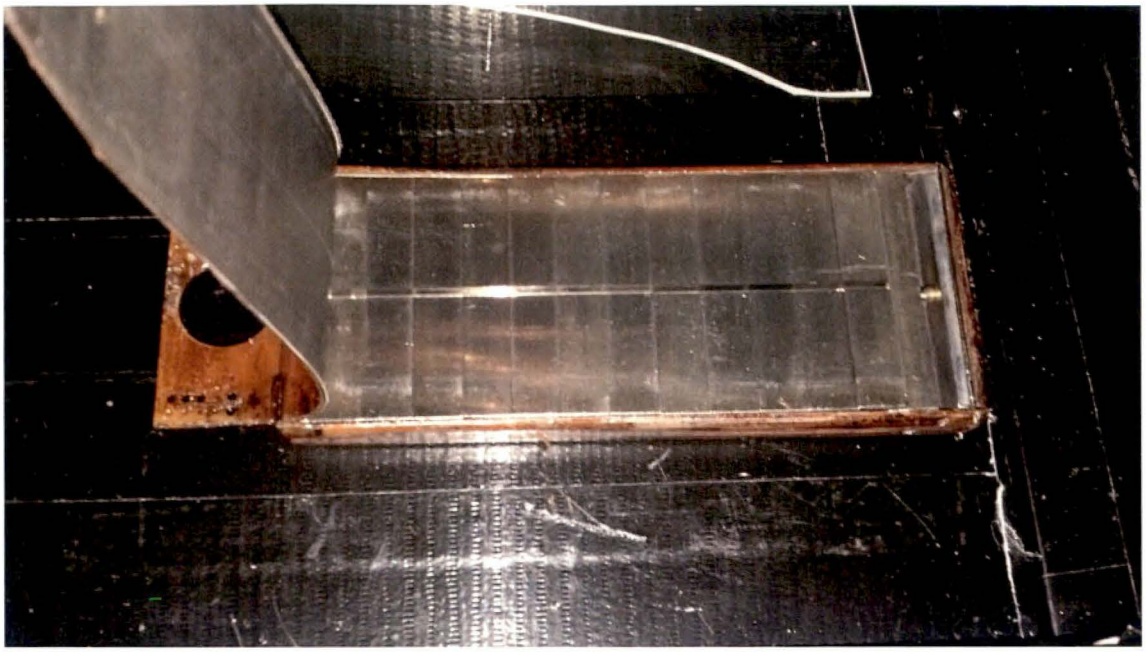

**Figure 2-10**
**Photograph of the Inside of the G1 Charpy Packet within the Peach Bottom Unit 2 30° Capsule**

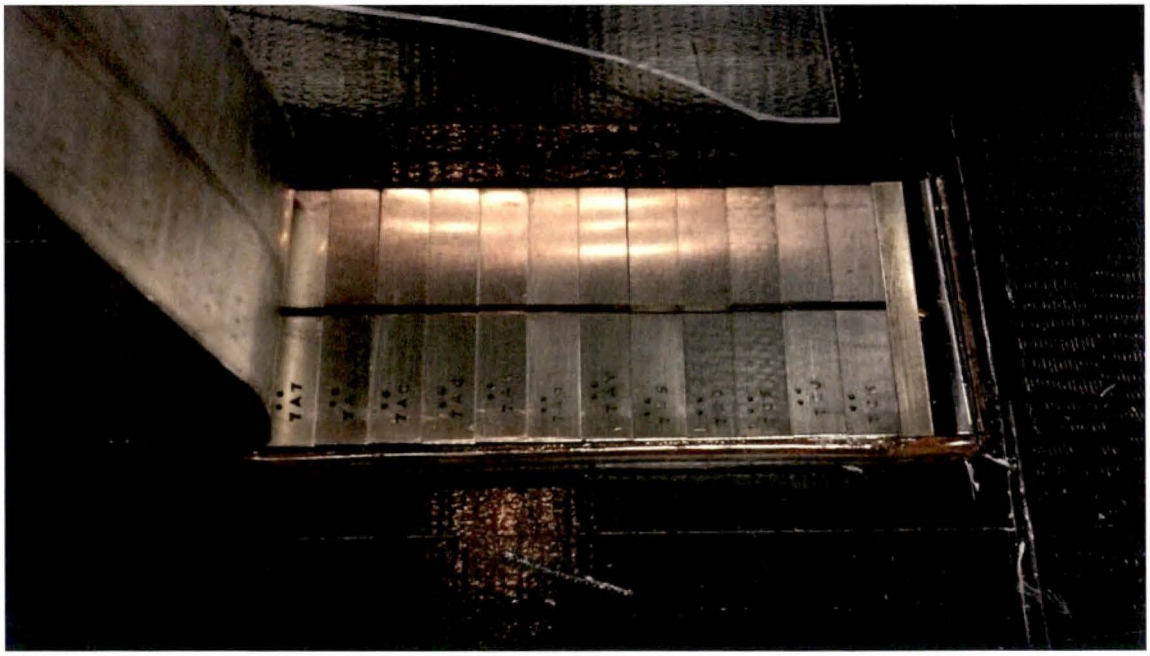

**Figure 2-11**
**Photograph of the Inside of the G2 Charpy Packet within the Peach Bottom Unit 2 30° Capsule**

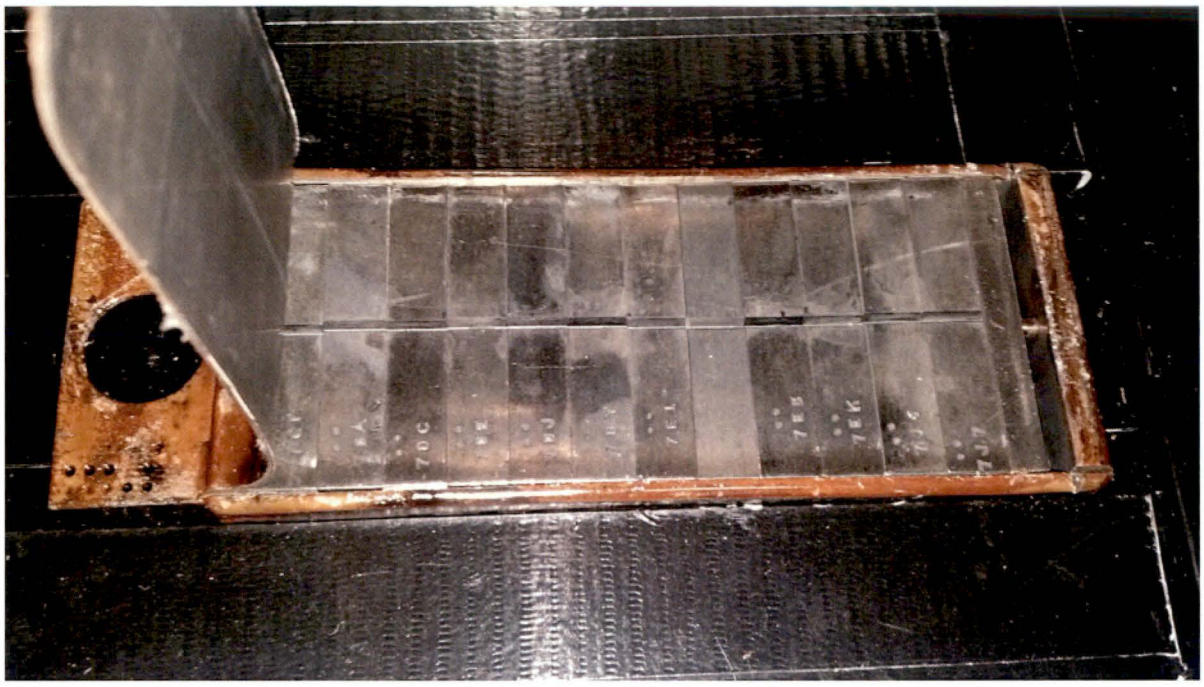

**Figure 2-12**
**Photograph of the Inside of the G3 Charpy Packet within the Peach Bottom Unit 2 30° Capsule**

# 3
# NEUTRON FLUENCE CALCULATION

This Section presents the results of an analysis to determine the dosimetry activity and fast neutron fluence in surveillance specimens removed from the Peach Bottom Unit 2 reactor. The computed activities are compared to measurements for the two irradiated surveillance capsules that were removed from the reactor. This surveillance capsule (30° location), which included iron, nickel, and copper flux wire dosimeters, had achieved an exposure of 33.6 effective full power years (EFPY) at the end of Cycle 22.

In addition to the 30° capsule evaluation, activities, and fluence were determined for the 120° surveillance capsule removed at the end of Cycle 7 (EOC 7). Table 3-1 summarizes the capsules pulled from the Peach Bottom Unit 2 reactor that are evaluated in this report.

**Table 3-1**
**Summary of the Peach Bottom Unit 2 Surveillance Capsules and Flux Wires**

| Capsule Location | Time of Removal | EFPY at Removal | Reference |
|---|---|---|---|
| 120° | EOC 7 | 7.5 | [8] |
| 30° | EOC 22 | 33.6 | - |

The determination of activation, fluence and combined uncertainty for the surveillance capsules and flux wires listed in Table 3-1 is based upon the RAMA Fluence Methodology [11], the RAMA Fluence Methodology Procedures Manual [12], and the RAMA Fluence Methodology Theory Manual [13].

The RAMA Fluence Methodology (hereinafter referred to as "RAMA") was developed by TransWare Enterprises Inc. under sponsorship of EPRI and the BWRVIP. In accordance with the requirements of U.S. Nuclear Regulatory Commission (NRC) Regulatory Guide 1.190, "Calculational and Dosimetry Methods for Determining Pressure Vessel Neutron Fluence" [14], RAMA is qualified against industry standard benchmarks for both boiling water reactor (BWR) and pressurized water reactor (PWR) designs. The RAMA methodology and TransWare's application of the methodology have been reviewed by the NRC and given generic approval for determining fast neutron fluence in both BWR and PWR pressure vessels [15] with no discernable bias in the computed results.

For BWR/4 class reactors, which includes Peach Bottom Unit 2, 233 surveillance measurements have been evaluated with an overall calculated-to-measured (C/M) comparison ratio and standard deviation of $1.03 \pm 0.12$.

## 3.1 Description of the Reactor System

This section provides an overview of the reactor design and operating data inputs that were used to develop the computational fluence model for the Peach Bottom Unit 2 reactor. All reactor design and operating data inputs used to develop the model are plant-specific and were provided by Exelon Generation Company, LLC. The inputs for the fluence geometry model were developed from nominal and as-built drawings for the RPV, RPV internals, fuel assemblies, and containment structures. The reactor operating history was also updated to provide a historical accounting of how the reactor operated for Cycles 1 through 22 with projections to end of license.

### *3.1.1 Overview of the Reactor System Design*

Peach Bottom Unit 2 is a General Electric BWR/4 class reactor with a core loading of 764 assemblies. The unit began commercial operation in 1974 with a design rated power of 3293 MWt. Multiple power uprates have occurred since initial startup. The timeline for when the uprates occurred and are projected to occur are presented in Section 3.1.4.2. At the time of this evaluation, Peach Bottom Unit 2 has completed 22 cycles of operation.

Figure 3-1 illustrates the basic planar configuration of the Peach Bottom Unit 2 reactor at an axial elevation near the reactor core mid-plane. All the radial regions of the reactor that are required for fluence evaluations are shown. Beginning at the center of the reactor and projecting outward, the regions include: the core region; core reflector region (bypass water); central shroud wall; downcomer water region including the jet pumps; RPV wall; cavity region between the RPV wall and insulation; insulation; cavity region between the insulation and biological shield; and the biological shield wall. Cladding is included on the inner RPV surface as well as the inner and outer surfaces of the biological shield wall. Also represented in Figure 3-1 are notations indicating the control rod and fuel assembly locations within the core. Note that the fuel locations are shown only for the northeast quadrant of the core region.

### *3.1.2 Reactor System Mechanical Design Inputs*

The mechanical design inputs used to construct the Peach Bottom Unit 2 fluence geometry model are based upon nominal design and as-built dimensional information. As-built data is preferred when constructing plant-specific reactor fluence models; however, as-built data is not always available and nominal dimensions are used.

For the Peach Bottom Unit 2 fluence model, the predominant dimensional information used to construct the fluence model is nominal design data. As-built dimensional data was used for the following reactor components:

- Top guide plate thickness

An important component of a computational reactor pressure vessel fluence model is the accurate description of the surveillance capsules installed in the pressure vessel. Figure 3-1 shows that the Peach Bottom Unit 2 reactor was initially equipped with three surveillance capsules. The surveillance capsules are distributed around the circumference of the pressure vessel at the 30°, 120° and 300° azimuths relative to the reactor north 0° angular direction. The capsules were installed at an elevation around the reactor core mid-plane. Each capsule was mounted radially near the inside surface (0T) of the RPV wall. The importance of surveillance

capsules in fluence analyses is that they contain flux wires that are irradiated during reactor operation. When a capsule is removed from the reactor, the irradiated flux wires are evaluated to obtain activity measurements. The measurements are used to validate the fluence model. At this time, it is noted that only the 30° and 120° surveillance capsules have been removed from the Peach Bottom Unit 2 reactor.

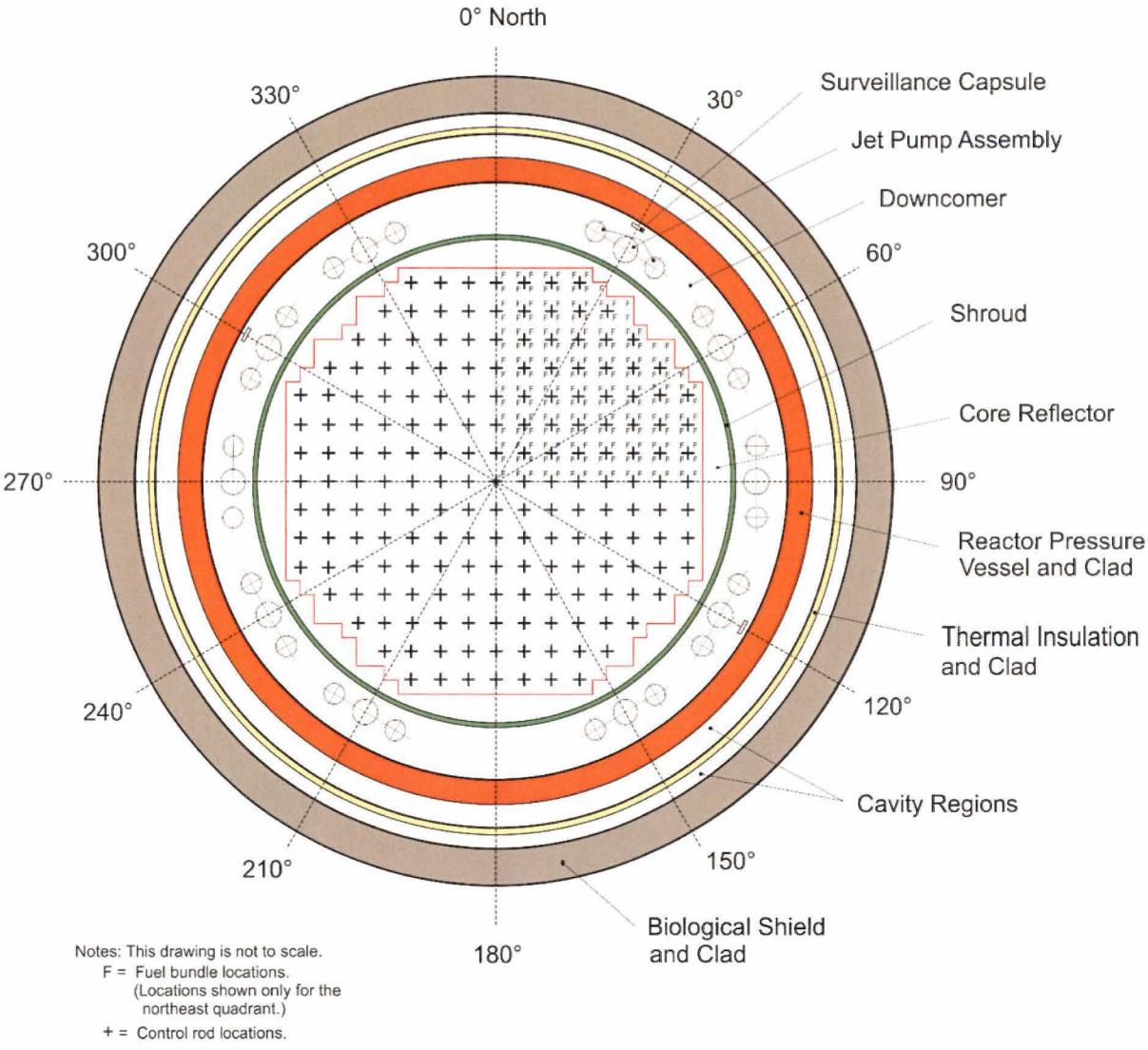


**Figure 3-1**
**Planar View of the Peach Bottom Unit 2 Reactor at the Core Mid-Plane Elevation**

### *3.1.3 Reactor System Material Compositions*

Each region of the reactor is comprised of materials that can include reactor fuel, metal, water, insulation, concrete, and air. Accurate material information is essential for the fluence evaluation as the material compositions determine the scattering and absorption of neutrons throughout the reactor system and, thus, affect the determination of neutron fluence in the RPV, surveillance capsules, vessel internal components, and ex-vessel structures.

Table 3-2 provides a summary of the materials for the principal components and regions of the Peach Bottom Unit 2 reactor. The material attributes for the metal, insulation, concrete, and air compositions (i.e., material densities and isotopic concentrations) are assumed to remain constant for the operating life of the reactor. The bulk water coolant properties throughout the reactor system, except for the core region, are determined assuming rated power and flow conditions. The coolant properties remain constant unless there is a reported change in system heat balance conditions that affect the water properties in the reactor. The nuclear fuel compositions and coolant properties in the reactor core region change continuously during reactor operation. The fuel and coolant properties in the core region are updated for each reactor statepoint condition based on the actual or predicted operating states of the reactor. Water properties immediately above and below the core region are updated on a cycle-by-cycle basis based on average cycle operating conditions.

**Table 3-2**
**Summary of Material Compositions by Region for Peach Bottom Unit 2**

| Region | Material Composition |
|---|---|
| Biological Shield Clad | Low-Alloy Steel |
| Biological Shield Wall | Reinforced Concrete |
| Capsule | Low-Alloy Steel |
| Cavity Regions | Air |
| Cruciform Control Rods | Stainless Steel, $B_4C$ |
| Capsule Flux Wire Holder Pipe | Stainless Steel |
| Capsule Flux Wire Holder Flow | Air |
| Control Rod Guide Tubes | Stainless Steel |
| Coolant | Water |
| Core | $^{235}U$, $^{238}U$, $^{239}Pu$, $^{240}Pu$, $^{241}Pu$, $^{242}Pu$, $O_{fuel}$, Zircaloy |
| Core Hardware | Zircaloy, Stainless Steel, Inconel, $B_4C$ |
| Core Support Plate & Hardware | Stainless Steel |
| Fuel Support Pieces | Stainless Steel |
| Insulation | Aluminum, Stainless Steel, Air |
| Insulation Cladding | Stainless Steel |
| Jet Pump Piping | Stainless Steel |
| Jet Pump Riser Brace Leaves | Stainless Steel |
| Jet Pump Riser Brace Pad | Stainless Steel |
| Jet Pump Riser Brace Yoke | Stainless Steel |
| Jet Pump Rams Head Beam | Inconel |

**Table 3-2 (continued)**
**Summary of Material Compositions by Region for Peach Bottom Unit 2**

| Region | Material Composition |
|---|---|
| Jet Pump Rams Head Bracket | Stainless Steel |
| LPRM Tube | Water |
| Nozzle Forgings | Low-Alloy Steel |
| RPV Clad | Stainless Steel |
| RPV Wall | Low-Alloy Steel |
| Shroud Wall | Stainless Steel |
| Shroud Head | Stainless Steel |
| Sparger Piping | Stainless Steel |
| Sparger Nozzles | Stainless Steel |
| Steam Separator Standpipes | Stainless Steel |
| Core Exit | Steam |
| Top Guide | Stainless Steel |
| Top Guide Pads | Stainless Steel |
| Top Guide Water | Water |

### *3.1.4 Reactor Operating Data Inputs*

An accurate evaluation of reactor vessel and component fluence requires an accurate accounting of the reactor's operating history. The principal operating parameters that affect the determination of neutron fluence in light water reactors include: core configurations, fuel assembly designs, power history, exposure and isotopic distributions, and water density distributions. The following subsections provide additional information on the characterization of reactor operating data for fluence evaluations.

#### 3.1.4.1 Core Configuration and Fuel Designs

The reactor core configuration and the fuel assembly designs loaded in the reactor determine the neutron source and spatial source distribution contributing to the irradiation of the pressure vessel, vessel internals and ex-vessel supporting structures. The Peach Bottom Unit 2 core is comprised of 764 fuel assemblies in a fixed configuration. Several designs of fuel assemblies may be loaded in the reactor core in any given operating cycle. In order to determine accurate spatial fluence profiles throughout the reactor system, it is important to account for the different fuel designs loaded in the reactor over the operating lifetime of the reactor, especially those designs that reside in the peripheral locations of the core region.

Table 3-3 provides a summary of the many fuel assembly designs that have been loaded in the Peach Bottom Unit 2 reactor core for each operating cycle evaluated in this report. Table 3-3 also identifies the dominant fuel design loaded on the core periphery for each cycle and indicates the dominant (most numerous) assembly present in **bold** font.

### 3.1.4.2 Reactor Power History

Reactor power history is the measure of reactor power levels, reactor power spatial distributions, fuel exposure distributions, and fuel isotopic distributions that a reactor experiences over its operating life. The power history data used in the Peach Bottom Unit 2 fluence evaluation includes daily power levels for Cycles 1 through 22. Projected operating data for Cycle 23 is used to project operating conditions to the reactor end of license. The power history for Peach Bottom Unit 2 also accounts for periods of reactor shutdown due to refueling outages and other events that affect the activation and decay of dosimetry data.

Table 3-4 provides a summary of the rated power history and EFPY per cycle for the Peach Bottom Unit 2 reactor. The accumulated EFPY is computed from the operating data provided by Exelon Generation Company, LLC and is verified against power production and exposure data obtained separately from plant records.

### 3.1.4.3 Reactor Statepoint Data

Statepoints break up operating history into ranges of operation based on similar power, exposure, and isotopic distributions. Typically, several statepoints are chosen for each cycle to represent the different operating conditions experienced by the reactor over the course of that cycle.

Core simulator data was provided by Exelon Generation Company, LLC to characterize the operating conditions of Peach Bottom Unit 2 for the historical Cycles 1 through 22 and projection Cycle 23. The data calculated with core simulator codes represents the best-available information about the reactor core's operating history over the reactor's operating life. In this analysis, the core simulator data provided by Exelon was processed by TransWare to generate statepoint data files for input to the fluence model.

Because core simulator codes are used for a variety of core analysis functions, 10's to 100's of core calculations may be performed to track and monitor the operation of a reactor over the course of an operating cycle. Not all core calculations are suitable for use in fluence evaluations. Therefore, each cycle of operating data is investigated to select the statepoints that are suitable for use in fluence evaluations. When all reactor conditions are considered, the number of core simulator statepoints selected for a fluence evaluation can vary appreciably from cycle to cycle.

A separate neutronics transport calculation is performed for each selected statepoint. The neutron fluxes calculated for each statepoint are then combined with the appropriate daily power history data described in Section 3.1.4.2 to provide an accurate accounting of the neutron fluence for the reactor pressure vessel, reactor vessel internals, and surveillance capsules. The periods of reactor shutdown are also accounted for in this process, particularly to allow for an accurate calculation of irradiated surveillance capsule activities.

**Table 3-3**
**Summary of Peach Bottom Unit 2 Core Loading Inventory**

| Cycle | 7x7 Designs | | 8x8 Designs | | | 9x9 Designs | | 10x10 Designs | | | | Dominant Peripheral Design |
|---|---|---|---|---|---|---|---|---|---|---|---|---|
| | GE3 | GE4 | GE5 GE6 GE7 | GE8 | GE9 | GE11 | ANF LTA | W LTA | GE13 | GE14 | GNF2 | |
| 1 | **764** | | | | | | | | | | | GE 7x7 |
| 2 | **576** | 184 | 4 | | | | | | | | | GE 7x7 |
| 3 | **404** | 356 | 4 | | | | | | | | | GE 7x7 |
| 4 | 144 | **356** | 264 | | | | | | | | | GE 7x7 |
| 5 | | 224 | **540** | | | | | | | | | GE 7x7 |
| 6 | | | **764** | | | | | | | | | GE 8x8 |
| 7 | | | **764** | | | | | | | | | GE 8x8 |
| 8 | | | **492** | 268 | 4 | | | | | | | GE 8x8 |
| 9 | | | **332** | 268 | 152 | 4 | 4 | 4 | | | | GE 8x8 |
| 10 | | | | **332** | 152 | 272 | 4 | 4 | | | | GE 8x8 |
| 11 | | | | 60 | 152 | **544** | 4 | 4 | | | | GE 8x8 |
| 12 | | | | | | **480** | | | 284 | | | GE 9x9 |
| 13 | | | | | | 188 | | | **576** | | | GE 9x9 |
| 14 | | | | | | | | | **472** | 292 | | GE 10x10 |
| 15 | | | | | | | | | 188 | **576** | | GE 10x10 |
| 16 | | | | | | | | | | **764** | | GE 10x10 |
| 17 | | | | | | | | | | **764** | | GE 10x10 |
| 18 | | | | | | | | | | **764** | | GE 10x10 |
| 19 | | | | | | | | | | **492** | 272 | GE 10x10 |
| 20 | | | | | | | | | | 204 | **560** | GE 10x10 |
| 21 | | | | | | | | | | | **764** | GE 10x10 |
| 22 | | | | | | | | | | | **764** | GE 10x10 |
| 23+ (1) | | | | | | | | | | | **764** | GE 10x10 |

1. Cycle 23+ was provided as a projection cycle. This cycle is assumed to be an equilibrium cycle for projecting fluence to the end of license.

**Table 3-4**
**Statepoint Data for Peach Bottom Unit 2 per Cycle Basis**

| Cycle Number | Rated Thermal Power (MWt) | Accumulated EFPY |
|---|---|---|
| 1 | 3293 | 1.3 |
| 2 | 3293 | 2.0 |
| 3(1) | 3293 | 2.8 |
| 4(1) | 3293 | 4.0 |
| 5(1) | 3293 | 5.2 |
| 6(1) | 3293 | 6.3 |
| 7 | 3293 | 7.5 |
| 8 | 3293 | 8.7 |
| 9 | 3293 | 9.8 |
| 10 | 3293 | 11.3 |
| 11 | 3458 | 13.1 |
| 12 | 3458 | 14.9 |
| 13 | 3458 | 16.7 |
| 14 | 3458 | 18.6 |
| 15(2) | 3458, 3514, 3496 | 20.4 |
| 16 | 3514 | 22.3 |
| 17 | 3514 | 24.2 |
| 18 | 3514 | 26.1 |
| 19 | 3514 | 28.0 |
| 20 | 3514 | 29.9 |
| 21 | 3951 | 31.7 |
| 22 | 4016 | 33.6 |
| 23+(3) | 4016 | 70.0 |

1. Detailed operating history information was not available for these cycles. Statepoints characterizing beginning-of-cycle, middle-of-cycle and end-of-cycle operating conditions were developed using bundle exposure distributions from cycle summary reports.
2. Cycle 15 had an uprate to 3514 MWt then a derate to 3496 MWt.
3. Cycle 23+ is assumed to be the equilibrium cycle for projecting fluence to the reactor end of license.

#### 3.1.4.4 Reactor Coolant Properties

The reactor coolant water densities used in the fluence model are determined using combinations of core simulator codes and reactor heat balance data.

The water densities used for the core inlet and the reactor core region are derived directly from the thermal-hydraulic calculations performed by core simulator codes. In general, core simulator codes provide active and bypass flow water density data for each fuel assembly in the core and incrementally along the axial height of the assembly as the coolant flows from core inlet to core exit. The water densities in the reflector region around the core, and inside the core shroud, are determined using the average pressure of the core region, assuming the water is a saturated liquid.

The water densities above the core, and specifically in the shroud upper plenum region, assume the steam quality exiting the core. There is no mixing of the exit steam with the unvoided or slightly voided bypass flow also exiting the core. This treatment of core exit water densities provides conservative conditions for determining fluence in the upper vessel components and for determining the upper elevation of the RPV beltline. The core exit steam is also used to fill the steam separator standpipes that extend above the shroud head.

The core spray sparger piping, which is present in the upper shroud plenum region, is filled with saturated water on the inside of the piping and is surrounded by the plenum core exit steam on the outside of the pipes.

The bulk water densities in the other regions of the reactor vessel are determined from plant-specific heat balance data. The water densities that are calculated in this manner include the jet pump flow, and feedwater. Heat balance data provides water properties in terms of temperature, pressure, and enthalpy assuming 100% power and flow operating conditions. The water densities determined at full power conditions remain constant throughout the cycle, and for all power states of the reactor throughout a cycle, which should be bounding for best-estimate fluence predictions.

## 3.2 Methodology

This section provides an overview of the methodology and modeling approach used to determine fast neutron fluence and activation for the Peach Bottom Unit 2 surveillance capsules.
The fluence model for Peach Bottom Unit 2 is a plant-specific model that is constructed from the design inputs described in Section 3.1. The computational tools used in the fluence and activation analyses are based on the RAMA Fluence Methodology (RAMA) software [11].
The RAMA Fluence Methodology is described in the RAMA Theory Manual [13]. A general approach for using the toolset is presented in the RAMA Procedures Manual [12].

### *3.2.1 Computational Method*

The RAMA Fluence Methodology is a system of computer codes, a data library, and an uncertainty methodology that determines best-estimate fluence and activations in light water reactor pressure vessels and vessel internal components. The primary software that comprises the methodology includes model builder codes, a particle transport code, and a fluence calculator code.

The primary inputs for the fluence methodology are mechanical design parameters and reactor operating history data. The mechanical design inputs are obtained from plant-specific design drawings, which include as-built measurements when available. The reactor operating history data is obtained from multiple sources, such as core simulator software, system heat balance calculations, daily operating logs, and cycle summary reports. A variety of outputs are available from the fluence methodology that include neutron flux, fast neutron fluence, dosimetry activation, and an uncertainty analysis.

The model builder codes consist of geometry and material processor codes that generate input for the RAMA transport code. The geometry model builder code uses mechanical design inputs and meshing specifications to generate three-dimensional geometry models of the reactor. The material processor code uses reactor operating data and material property inputs to process fuel materials, structural materials, and water densities that are consistent with the geometry meshing generated by the geometry model builder code.

The RAMA transport code performs three-dimensional neutron flux calculations using a deterministic, multigroup, particle transport theory method with anisotropic scattering that is based upon the Method of Characteristics [16]. The transport solver is coupled with a general geometry modeling capability based on combinatorial geometry techniques. The coupling of general (arbitrary) geometry with a deterministic transport solver provides a flexible, efficient, and stable method for calculating neutron flux in light water reactor pressure vessels, vessel components, and structures. The primary inputs for the transport code include the geometry and material data generated by the model builder codes and numerical integration and convergence parameters for the iterative transport calculation. The primary output from the transport code is the neutron flux in multigroup form for every material region mesh in the fluence model.

The fluence calculator code determines fluence and activation in the reactor pressure vessel, surveillance specimens, and vessel components over specified periods of reactor operation. The fluence calculator also includes treatments for isotopic production and decay that are required to calculate specific activities for irradiated materials, such as the dosimetry specimens in the surveillance capsules. The primary inputs to the fluence calculator include the multigroup neutron flux from the transport code, response functions for the various materials in the reactor, reactor power levels for the operating periods of interest, specification of which components to evaluate, and the energy ranges of interest for evaluating neutron fluence. The reactor operating history is generally represented with several reactor statepoints that represent the core power and core power distributions of the reactor over the operating life of the reactor. These statepoints are integrated with the daily variations in reactor power levels to predict the fluence and activations accumulated throughout the reactor system.

The RAMA nuclear data library contains atomic mass data, nuclear cross-section data, response functions, and other nuclear constants that are needed for each of the code tools. The structure and contents of the data contained within the nuclear data file are based on the BUGLE-96 nuclear data library [17], with extended data representations derived from the VITAMIN-B6 data library [18].

The uncertainty methodology provides an assessment of the overall accuracy of the fluence and activation calculations. Variations in the dimensional data, reactor operating data, dosimetry measurement data, and nuclear data are evaluated to determine if there is a statistically significant bias in the calculated results that might affect the determination of the best-estimate

fluence for the reactor. The plant-specific results are also weighted with comparative results from experimental benchmarks and other plant analyses and analytical uncertainties pertaining to the methodology to determine if the plant-specific model under evaluation is statistically acceptable as defined in Regulatory Guide 1.190 [14].

### *3.2.2 Fluence Model*

Section 3.1 describes the design inputs that were provided for constructing the Peach Bottom Unit 2 reactor fluence model. These design inputs are used to develop a plant-specific, three-dimensional computer model of the Peach Bottom Unit 2 reactor for determining fast neutron fluence and activation in the reactor dosimetry specimens.

Figures 3-2 and 3-3 provide general illustrations of the primary components, structures, and regions developed for the Peach Bottom Unit 2 fluence model. Figure 3-2 shows the planar configuration of the reactor model at an elevation corresponding to the reactor core mid-plane elevation. Figure 3-3 shows an axial configuration of the reactor model. Note that the figures are not drawn to scale and do not include representations of the meshing developed for this evaluation. The figures are intended only to provide a perspective for the layout of the model, and specifically how the various components, structures, and regions lie relative to the reactor core region (i.e., the neutron source). Additional detail is beyond the scope of this document.

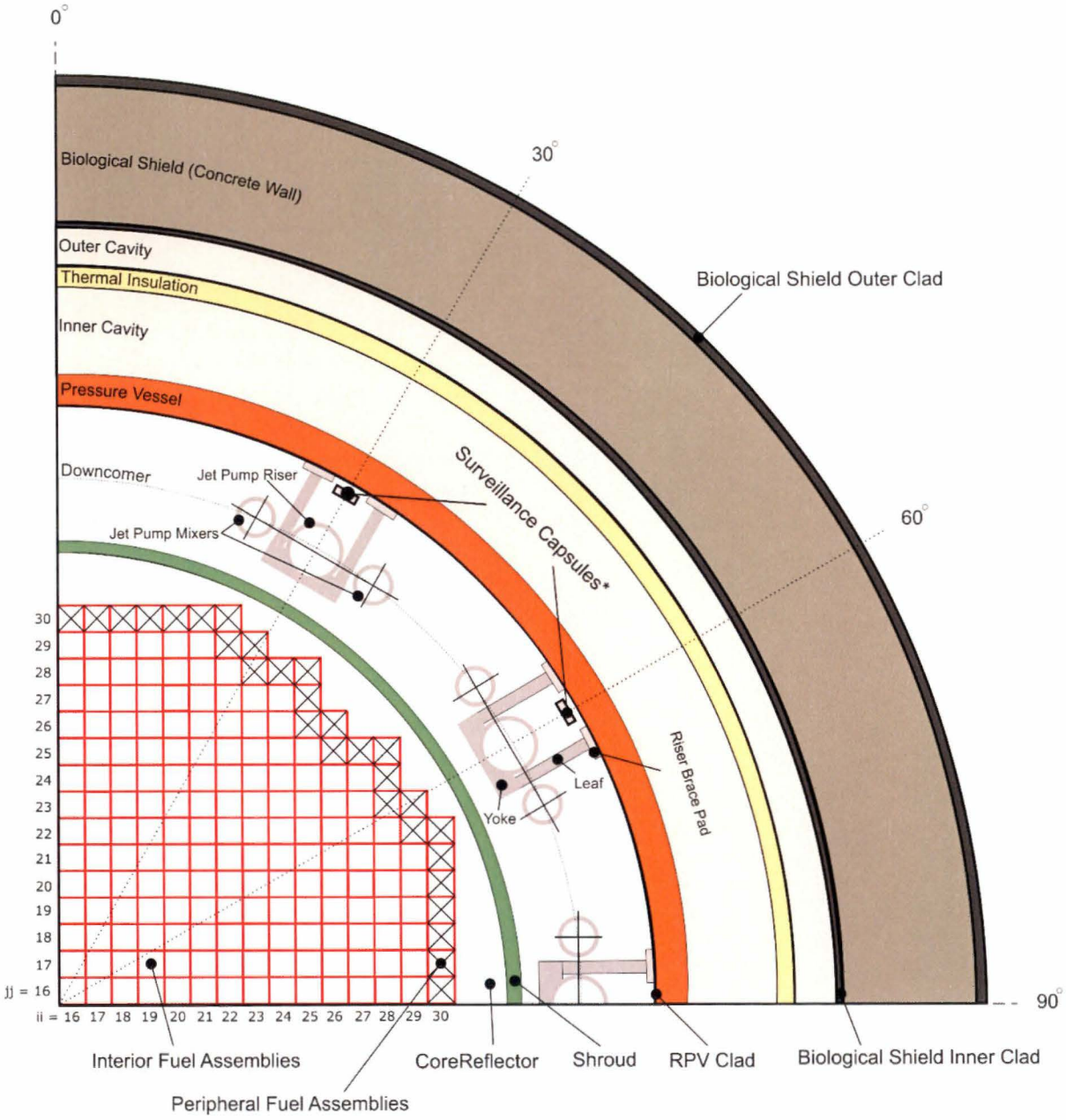


Notes: This drawing is not to scale.
* In quadrant symmetry, these capsules represent the 30°, 120° and 300° capsules

**Figure 3-2**
**Planar View of the Peach Bottom Unit 2 Fluence Model at the Core Mid-Plane Elevation in Quadrant Symmetry**

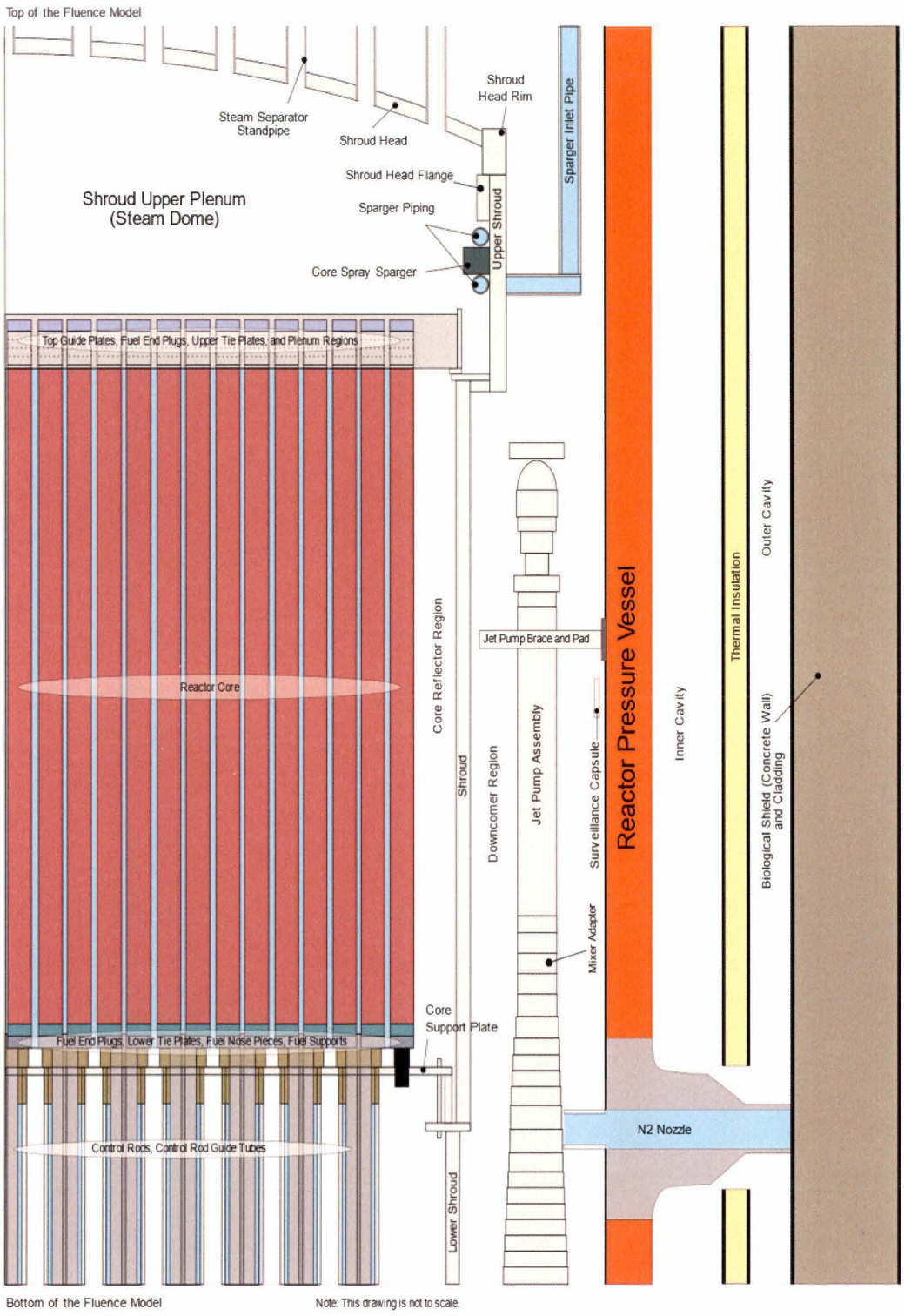


**Figure 3-3**
**Axial View of the Peach Bottom Unit 2 Fluence Model**

### 3.2.2.1 Geometry Model

The Peach Bottom Unit 2 fluence model is constructed on a Cartesian coordinate system using a generalized three-dimensional geometry modeling technique based on combinatorial geometry. The axial plane of the reactor model is defined by the (x,y) coordinates of the modeling system and the axial elevation at which a plane exists is defined along a perpendicular z-axis of the modeling system. This allows any point in the reactor model to be referenced by specifying the (x,y,z) coordinates for that point.

The geometry modeling system allows for solid body elements to be constructed to describe the various components, regions, and structures of the reactor. The primary elements ("primitives") used to construct the fluence model include rotatable boxes, cylinders, parallelepipeds, truncated cones, spheres, approximated toroids, and wedges. This modeling approach permits a model to be developed in any level of high-definition detail, such as is necessary for fluence and activation evaluations.

Figure 3-1 illustrates a planar cross-section view of the Peach Bottom Unit 2 reactor design at an axial elevation corresponding to the reactor core mid-plane. It is shown for this one elevation that the reactor design is a complex geometry composed of various combinations of rectangular, cylindrical, and wedge-shaped bodies. When the reactor is viewed in three dimensions, the varying heights of the different components, structures, and regions create additional geometry modeling complexities. An accurate representation of these geometrical complexities in a predictive computer model is essential for calculating accurate, best-estimate fluence in the reactor pressure vessel, surveillance capsules, vessel internals, and the supporting structures inside and outside of the reactor vessel.

Figure 3-2 and Figure 3-3 provide general illustrations of the planar and axial geometry complexities that are represented in the fluence model. For comparison purposes, the planar view illustrated in Figure 3-2 corresponds to the core elevation illustrated in Figure 3-1. The fluence model assumes reflective azimuthal quadrant symmetry in the planar dimension.

Figure 3-2 illustrates the quadrant geometry that is modeled in this analysis. In terms of the modeling coordinate system, this quadrant is designated the "northeast" quadrant of the reactor system. The 0-degree azimuth, which has a "north" designation, corresponds to the 0-degree azimuth referenced in the plant drawings for the reactor pressure vessel. Azimuthal position is incremented clockwise, resulting in the 90-degree azimuth being designated as the "east" direction.

Figure 3-3 illustrates the axial configuration of the primary components, structures, and regions in the fluence model. The figure shows that the axial height of the fluence model spans from a lower elevation below the recirculation nozzles to above the core shroud head. Although not explicitly shown in the Figure 3-3, the model includes the N1 recirculation outlet nozzles.

As previously noted, Figure 3-2 and Figure 3-3 are not drawn precisely to scale and are intended only to provide a perspective of how the various components, structures, and regions of the reactor are positioned relative to the reactor core region. The following subsections provide additional information on the constituent models developed for the individual components, structures, and regions of the fluence model.

### 3.2.2.2 Reactor Core and Core Reflector

The reactor core contains the nuclear fuel that is the source of the neutrons that irradiate all components and structures of the reactor. The core is surrounded by a shroud structure that serves to channel the reactor coolant through the core region during reactor operation. The coolant-containing region between the core and the core shroud is the core reflector. The reactor core geometry is rectangular in design and is modeled with rectangular elements to preserve its shape in the analysis. The core reflector region interfaces with the rectangular shape of the core region and the curved shape of the core shroud. It is, therefore, modeled using a combination of rectangular and cylindrical elements.

The core region is centered in the reactor pressure vessel and is radially-characterized in the analysis with two fundamental fuel zones: interior fuel assemblies and peripheral fuel assemblies. The peripheral fuel assemblies are the primary contributors to the neutron source in the fluence calculation. Because these assemblies are loaded at the core edge where neutron leakage from the core is greatest, there is a sharp power gradient across these assemblies that requires consideration. To account for the power gradient, the peripheral fuel assemblies are sub-meshed with additional elements that approximate the pin-wise details of the fuel assembly geometry and power distribution within the pins. The interior fuel assemblies make a lesser contribution to the reactor fluence and are, therefore, modeled in various homogenized forms in accordance with their contributions to the reactor fluence. For computational efficiency, homogenization treatments are used in the interior core region primarily to reduce the number of mesh regions that must be solved in the transport calculation. The meshing configuration for each fuel assembly location in the core region is determined by parametric studies to ensure an accurate estimate of neutron flux and fluence throughout all regions of the reactor system.

Each fuel assembly design, whether loaded in the interior or peripheral locations in the core, is represented with five axial material zones: the fuel nose piece zone, the fuel lower tie plate/end plug zone, the fuel zone, the fuel upper plenum zone, and the fuel upper tie plate/end plug zone. The structural materials in the top and bottom regions for each unique assembly design are represented in the model to address the shielding effects that these materials have on the components above and below the core region. The fuel zone contains the nuclear fuel and structural materials for the fuel assemblies. Because the composition of the fuel materials varies with core exposure (i.e., burnup) and by cycle (e.g., core loading), each fuel location in the reactor core is represented uniquely in the fluence model.

### 3.2.2.3 Reactor Core Shroud

The core shroud is a canister-like structure that surrounds the reactor core. It channels the reactor coolant and steam produced by the core into the steam separators. Axially the shroud extends almost the entire height of the model and is divided into three sections: lower, central, and upper. The lower shroud extends from the bottom of the model to the core support plate flange, the central shroud extends from the core support plate flange to the top guide flange, and the upper shroud extends from top guide flange to the top of the shroud head rim.

The shroud structure is illustrated in Figure 3-3. It is shown that the shroud wall and flanges are cylindrical in design and are accurately modeled with cylindrical elements. The shroud head contains spherical and pipe regions and are accurately modeled with spherical and pipe elements.

Above the shroud wall is the shroud head which is penetrated by numerous steam separator standpipes. The shroud head is semi-spherical in design and is modeled with spherical elements. The standpipes channel the steam produced in the core into the steam separators. The steam separator standpipes are cylindrical in design and are modeled with cylindrical elements.

#### 3.2.2.4 Downcomer Region

The downcomer region lies between the core shroud and the reactor pressure vessel. The downcomer is effectively cylindrical in design, but with geometrical complexities created by the presence of jet pumps and surveillance capsules in the region. The majority of the downcomer region is modeled with cylindrical elements. The areas of the downcomer containing the jet pumps and surveillance capsules are modeled with the appropriate geometry elements to represent their design features and to preserve their radial, azimuthal, and axial placement in the downcomer region. These structures are described further in the following subsections.

##### *3.2.2.4.1 Jet Pumps*

Peach Bottom Unit 2 has ten jet pump assemblies in the downcomer region, which provide the main recirculation flow for the core. In the fluence model, jet pump assemblies are positioned azimuthally at 30°, 60°, and 90°, which when symmetry is applied to the model, represents all ten jet pumps in the reactor. The 30° jet pump represents the 30°, 150°, 210° and 330° jet pumps; the 60° jet pump represents the 60°, 120°, 240° and 300° jet pumps; and the 90° jet pump represents the 90° and 270° jet pumps. Note there are no jet pumps present at the 0° or 180° locations.

The jet pump assembly model includes representations for the riser, mixer, and diffuser pipes, nozzles, rams head, riser inlet pipe, and riser brace yoke, leaves and pads. The jet pump assembly is modeled using cylindrical elements for the jet pump riser and mixer pipes. The mixer nozzles, adapters, and diffusers are modeled as stepped shells to represent the axially-varying radii. The riser pipe is correctly situated between the mixer pipes. Holding the riser pipe in place are riser brace elements, which are approximated as rectangular regions by radially segmented cylindrical arc elements. The jet pump assembly includes hold down beams and brackets, built with rectangular elements that are attached to the ram's head. Toroidal elements are used to model the rams head piping.

##### *3.2.2.4.2 Surveillance Capsules*

Section 3.1 describes the surveillance capsules installed in the Peach Bottom Unit 2 reactor. The three (3) OEM surveillance capsules installed in the Peach Bottom Unit 2 reactor are positioned in close proximity to the RPV inner wall surface at the 30°, 120° and 300° azimuthal angles around the pressure vessel. For this analysis, which assumes quadrant symmetry in the azimuthal dimension, the capsule modeled at 30° represents the 30° capsule and the 60° capsule represents the 120° and 300° capsules in the reactor. A separate flux wire holder is attached externally to the 30° surveillance capsule container. Although the flux wire holder is not shown in the figures of this report, it is included in the model and is represented at the 30° capsule location.

The vessel surveillance capsules are rectangular in design but are approximated in the model with cylindrical elements to facilitate their inclusion in the cylindrical geometry that defines the downcomer region model. This modeling approximation is acceptable due to the small view

factor of the capsule relative to its radial distance from the reactor core. The coolant water that surrounds the capsule containers on all sides is explicitly modeled for its scattering and attenuation effects in the neutronics calculation.

#### 3.2.2.5 Reactor Pressure Vessel

The reactor pressure vessel and vessel cladding lie outside the downcomer region, with both modeled using cylindrical elements. The cladding-pressure vessel interface is a key location for RPV fluence calculations and is preserved in the model. This interface defines the inside surface (0T) for the pressure vessel base metal where the RPV fluence is calculated. Peach Bottom Unit 2 has cladding only on the inside surface of the pressure vessel wall.

Representations of the forgings for the recirculation inlet (N2) and outlet (N1) nozzles are included in the RPV wall. The nozzle forgings and safe-ends extend radially outward into the cavity region to the biological shield wall. These nozzle representations are modeled in their true cylindrical forms using cylindrical and conical elements to preserve their basic design features. The instrumentation (N16) nozzle's small diameter is approximated by editing fluence directly from the RPV wall.

#### 3.2.2.6 Thermal Insulation

The reactor vessel thermal insulation lies in the cavity region outside the pressure vessel wall. The insulation is cylindrical in design and follows the contour of the pressure vessel wall. It is modeled with cylindrical elements.

#### 3.2.2.7 Inner and Outer Cavity

There are effectively two cavity regions represented in the model. The inner cavity region lies between the outer surface of the pressure vessel wall and the inner surface of the vessel insulation. The outer cavity region lies between the outer surface of the vessel insulation and inner surface of the biological shield wall cladding. The cavity regions follow the cylindrical contours of the pressure vessel wall, vessel insulation, and biological shield, and are therefore modeled with cylindrical elements.

#### 3.2.2.8 Biological Shield Model

The biological shield (concrete) defines the outermost region of the fluence model. The biological shield for the modeled elevations is effectively cylindrical in design and is modeled with cylindrical elements. Cladding is modeled on the inside and outside surfaces of the concrete wall.

#### 3.2.2.9 Above-Core Components

Figure 3-3 includes illustrations of other components and regions that lie above the reactor core region. The predominant above-core components represented in the model include the top guide, core spray spargers, upper core shroud wall, shroud head, and steam separator standpipes. The shroud regions and standpipes are mentioned in further detail in Section 3.2.2.3.

#### 3.2.2.9.1 Top Guide

The top guide component lies above the core region and is appropriately modeled to include discrete representations of the top guide plates and accounting for the fuel assembly parts, top guide pads, and coolant between the plates. The fuel assembly parts are modeled in two axial segments: the fuel rod plenum and the fuel assembly upper tie plate, which includes the fuel rod upper end plugs. The top guide is modeled with combinations of rectangular and cylindrical elements. The top guide pads are approximated as cylindrical elements. The fuel assembly parts are modeled with the elements of the reactor core region.

#### 3.2.2.9.2 Core Spray Spargers and Piping

The core spray spargers include upper and lower sparger annulus pipes and a vertical inlet pipe. The core spray spargers are appropriately represented as torus structures in the model. The sparger pipes reside inside the upper shroud wall above the top guide. The spargers are modeled as pipe-like structures and include a representation of reactor coolant inside the pipes. The sparger spray nozzles are not represented individually. Instead, the region in which they reside is represented as a homogeneous cylinder comprised of steam and stainless steel.

### 3.2.2.10 Below-Core Component Models

Figure 3-3 includes illustrations of other components and regions that lie below the reactor core region. The predominant below core (i.e., below active fuel) components represented in the fluence model include the lower fuel assembly parts, fuel support pieces, core support plate, core support plate rim bolts, cruciform control rods, control rod guide tubes, and lower shroud wall. The lower shroud wall and fuel assembly components are described in previous sections, with the remaining components described in the following subsections.

#### 3.2.2.10.1 Core Support Plate and Rim Bolts

The core support plate includes appropriate penetrations for the fuel support pieces, control rod guide tubes, cruciform control rods, and the core support plate rim bolts. Core support plate rim bolts protrude from the top of the core support plate and traverse through the plate, rim, and core shroud lower flange. The core support plate and rim are modeled using cylindrical and rectangular elements, while the rim bolts are modeled by cylindrical elements.

#### 3.2.2.10.2 Fuel Support Pieces

The nuclear fuel assemblies loaded in the reactor are seated on fuel support pieces, which then rest in the core support plate and control blade guide tubes. Two types of fuel support pieces are included in the fluence model: a four-assembly fuel support piece, and a single-assembly fuel support piece for peripheral assembly locations. The four-assembly fuel support piece allows for the presence of a cruciform control rod and the associated coolant flow. Combinations of cylindrical, rectangular, and wedge elements are used to construct the fuel support piece models.

#### *3.2.2.10.3 Control Blades and Guide Tubes*

The fluence model allows for the representation of cruciform-shaped control blades and tubular control blade guide tubes in the below-core regions of the reactor. Coolant flow paths are included in the model to account for the scattering of neutrons in the subcooled water regions outside the guide tube and around the control blade inside the guide tube. The control blade and guide tube components are modeled using combinations of rectangular and cylindrical elements.

### 3.2.2.11 Summary of the Geometry Modeling Approach

To summarize the reactor modeling process, there are several key features that allow the reactor design to be accurately represented for capsule fluence evaluations. Following is a summary of some of the key features of the model:

- Combinations of rectangular, cylindrical, conical, spherical, toroidal, and wedge elements are used in the model to provide an accurate geometrical representation of the components, structures, and regions in the reactor.
- The reactor core is modeled with rectangular and wedge elements to represent the true geometrical shape of the core. The fuel assemblies in the core region are also sub-meshed with additional rectangular and wedge elements to represent the power and isotopic distributions in the assemblies.
- The fuel assembly tie plates, fuel rod end plugs, fuel nose piece, fuel channel and bypass flow regions are appropriately represented above and below the active fuel elevations. These components and regions are modeled using the same geometry elements as the reactor core.
- A combination of rectangular and cylindrical elements are used to describe the transition parts between the rectangular boundary of the core region and the cylindrical boundary of the core shroud.
- Cylindrical, conical, and wedge elements are used to model the components and regions that extend outward from the core region (core shroud, downcomer, RPV, etc.).
- Each jet pump assembly in the downcomer region includes appropriate representations for the riser pipe, mixer pipes, diffuser pipes, nozzles, couplers, rams head, hold down bracket, riser brace and yoke assembly, riser brace pads, etc. and are modeled using combinations of cylindrical, box, conical and wedge elements.
- The reactor vessel surveillance capsules are modeled with arc elements at their nominal radial, azimuthal, and elevational positions behind the jet pumps in the downcomer region. Using azimuthal symmetry conditions, all surveillance capsules are represented in the quadrant-symmetric fluence model.
- The above-core region includes accurate representations of the top guide, upper fuel assembly parts, core spray spargers and piping, upper core shroud, shroud head, and steam separator standpipes. Combinations of rectangular parallelepiped, cylindrical, spherical, toroidal, and wedge elements are used to describe the above-core components and coolant regions.

- The below-core region includes appropriate representations for the lower fuel assembly parts, fuel support pieces, core support plate, core support plate rim bolts, core coolant inlet regions, cruciform control rods, and control rod guide tubes. Combinations of rectangular parallelepiped, cylindrical, spherical, toroidal, and wedge elements are used to describe the below-core components and coolant regions.
- The biological shield is appropriately represented as a cylinder with cladding on the inside and outside surfaces of the biological shield wall. The biological shield is described with cylindrical elements.

### *3.2.3 Parametric Sensitivity Analyses*

Several plant-specific sensitivity analyses are performed to evaluate the accuracy and predictability of the neutral particle transport methodology for determining RPV fluence. Geometric meshing and numerical integration parameters are among the items pre-evaluated to ensure that the transport solution provides consistent results in all azimuthal, radial and axial dimensions of the reactor fluence model. The ultimate validation of the model is the demonstration that predicted activations for reactor surveillance dosimetry and boat samples, if available, meet the requirements of Regulatory Guide 1.190.

### *3.2.4 Particle Transport Calculation Parameters*

The accuracy of the transport method is based on a numerical integration technique that employs ray-tracing to characterize the geometry, anisotropy treatments to determine the density and directional flow (i.e., angular flux) of particles, and convergence parameters to determine the overall accuracy of the converged flux. Plant-specific values are determined for each significant integration and ray-tracing parameter.

Two key parameters for the calculation of accurate angular flux are the angular quadrature set and Legendre order of scattering used in the transport calculation. The importance of the angular quadrature set is specifically addressed in Regulatory Position 1.3.5 of Regulatory Guide 1.190, where it is cited that an $S_8$ angular quadrature (which is used in traditional transport models) may not be adequate when used in cavity transport calculations. The fluence model used in this analysis employs a higher-order $S_{10}$ angular quadrature for all transport calculations to improve computational accuracy over the extended RPV beltline region.

The transport calculations also use the highest order of Legendre expansion of the scattering cross sections that is available on the nuclear data library for the anisotropy treatment. For the actinide and zirconium nuclides, this corresponds to a $P_5$ expansion of the scattering cross sections, while for all other nuclides, a $P_7$ expansion of the scattering cross sections is used.

Additional parameters of the calculation control the saturation of rays throughout the geometry by means of the parallel and axial ray densities as well as ray depths. The overall accuracy of the neutron flux calculation is determined using an iterative technique that converges the particle fluxes in all regions of the transport model.

### *3.2.5 Fission Spectrum and Neutron Source*

Modern core simulator software is capable of providing three-dimensional core power distributions and fuel isotopics in high-definition detail, viz., on a pin-by-pin basis. This allows fluence models to be constructed with a high-level of modeling detail for representing unique fission spectrum and neutron source terms for the transport calculation. This detail is incorporated into the fluence model.

The fission spectrum is determined for each transport calculation based on the relative weights of the $^{235}U$, $^{238}U$, $^{239}Pu$, $^{240}Pu$, $^{241}Pu$ and $^{242}Pu$ isotopes in the fuel materials. The fission spectra for the uranium and plutonium isotopes are derived from information that is provided in the BUGLE-96 nuclear data library [17] and the VITAMIN-B6 data library [18].

The spatial neutron source distribution is determined for each transport calculation using the pin wise power density factors obtained from the core simulator software and data from the nuclear data library.

For fluence evaluations, the peripheral fuel assemblies are specifically modeled to preserve the pin-wise power gradient at the core edge, as these bundles have the greatest effect on the determination of fluence in the reactor pressure vessel.

## 3.3 Surveillance Capsule Activation and Fluence Results

This section documents the activation analysis that was performed for the Peach Bottom Unit 2 surveillance capsules. The activation results form the basis for the validation and qualification of the fluence methodology as applied to the Peach Bottom Unit 2 reactor in accordance with the Regulatory Guide 1.190 [14]. Regulatory Guide 1.190 requires fluence calculational methods to be validated by comparisons with measurements from operating reactor dosimetry for the specific reactor being evaluated, or from reactors with similar design. The acceptance criteria provided in Regulatory Guide 1.190 is that the comparison-to-measurement (C/M) and standard deviation values must be less than or equal to 20%. The Peach Bottom Unit 2 reactor capsule measurement comparisons meet the Regulatory Guide 1.190 criteria and, as such, no bias adjustment is required to be applied to the computed RPV fluence.

### *3.3.1 Summary of the Flux Wire Activation Analysis*

Two OEM surveillance capsules located at the 30° and 120° azimuths have been removed from the Peach Bottom Unit 2 reactor. Activation measurements were performed for the flux wires extracted from the capsule and a comparison of calculated activities to measurements are presented in this report. Table 3-5 provides a summary of the activation comparisons and fast neutron fluence ($E > 1.0$ MeV) determined for the capsules removed from Peach Bottom Unit 2 reactor.

**Table 3-5**
**Summary of Fluence and Activity Comparisons for the Peach Bottom Unit 2 Dosimetry**

| Dosimeter | Time of Removal | Accumulated Exposure (EFPY) | Fast Neutron Fluence (>1.0 MeV, n/cm$^2$) | Number of Measurements | Calculated vs. Measured (C/M) | Standard Deviation (σ) |
|---|---|---|---|---|---|---|
| 120° Capsule | EOC 7 | 7.5 | 2.59E+17 | 6 | 1.07 | 0.07 |
| 30° Capsule | EOC 22 | 33.6 | 9.13E+17 | 9 | 1.19 | 0.08 |

### *3.3.2 Comparison of Predicted Activation to Plant-specific Measurements*

The comparison of predicted activations to measurements for the Peach Bottom Unit 2 Cycle 7 and Cycle 22 flux wires are presented in this subsection. Fluence and lead factors for each capsule are reported in Subsection 3.3.3.

#### 3.3.2.1 Cycle 7 120° Surveillance Capsule Activation Analysis

Copper, iron, and nickel flux wires were irradiated in the Peach Bottom Unit 2 120° surveillance capsule during the first seven cycles of reactor operation. The wires were removed after being irradiated for a total of 7.5 EFPY [8]. Activation measurements were performed for the following reactions: $^{63}$Cu (n,α) $^{60}$Co, 58Ni (n,p) $^{58}$Co, and $^{54}$Fe (n,p) $^{54}$Mn. The precise location of the individual wires within the capsule is not known; therefore, the activation calculations were performed at the center of the capsule container.

Table 3-6 provides a comparison of the calculated specific activities and the measured specific activities for each flux wire specimen. The average calculated-to-measured (C/M) ratio and standard deviation for the flux wires irradiated in the 120° capsule is determined to be 1.07 ± 0.07.

**Table 3-6**
**Comparison of Flux Wire Calculated-to-Measured Activities for the 120° Surveillance Capsule Removed from Peach Bottom Unit 2 at EOC 7**

| Flux Wires | Measured (dps/mg) | Calculated (dps/mg) | Calculated vs. Measured (C/M) | Standard Deviation (σ) |
|---|---|---|---|---|
| **Iron** | | | | |
| **64945** | 5.74E+04 | 6.60E+04 | 1.15 | — |
| **64946** | 6.13E+04 | 6.60E+04 | 1.08 | — |
| **Iron Average** | — | — | 1.11 | 0.05 |
| **Nickel** | | | | |
| **64945** | 1.14E+06 | 1.28E+06 | 1.12 | — |
| **64946** | 1.16E+06 | 1.28E+06 | 1.10 | — |
| **Nickel Average** | — | — | 1.11 | 0.01 |
| **Copper** | | | | |
| **64945** | 8.36E+03 | 8.22E+03 | 0.98 | — |
| **64946** | 8.49E+03 | 8.22E+03 | 0.97 | — |
| **Copper Average** | — | — | 0.98 | 0.01 |
| **Total Flux Wire Average** | — | — | **1.07** | **0.07** |

### 3.3.2.2 Cycle 22 30° Surveillance Capsule Activation Analysis

Copper, iron, and nickel flux wires were irradiated in the Peach Bottom Unit 2 30° surveillance capsule during the first twenty-two cycles of reactor operation. The wires were removed after being irradiated for a total of 33.6 EFPY. Activation measurements were performed for the following reactions: $^{63}$Cu (n,α) $^{60}$Co, 58Ni (n,p) $^{58}$Co, and $^{54}$Fe (n,p) $^{54}$Mn. The precise location of the individual wires within the capsule is not known; therefore, the activation calculations were performed at the center of the capsule container.

Table 3-7 provides a comparison of the calculated specific activities and the measured specific activities for each flux wire specimen. The average calculated-to-measured (C/M) ratio and standard deviation for the flux wires irradiated in the 30° capsule is determined to be 1.19 ± 0.08.

**Table 3-7**
**Comparison of Flux Wire Calculated-to-Measured Activities for the 120° Surveillance Capsule Removed from Peach Bottom Unit 2 at EOC 22**

| Flux Wires | Measured (dps/g) | Calculated (dps/g) | Calculated vs. Measured (C/M) | Standard Deviation (σ) |
|---|---|---|---|---|
| **Iron** | | | | |
| **G1** | 75.03 | 90.57 | 1.21 | — |
| **G2** | 74.83 | 90.57 | 1.21 | — |
| **G3** | 76.04 | 90.57 | 1.19 | — |
| **Iron Average** | — | — | 1.20 | 0.01 |
| **Nickel** | | | | |
| **G1** | 901.09 | 1154.36 | 1.28 | — |
| **G2** | 901.11 | 1154.36 | 1.28 | — |
| **G3** | 898.15 | 1154.36 | 1.29 | — |
| **Nickel Average** | — | — | 1.28 | 0.00 |
| **Copper** | | | | |
| **G1** | 11.74 | 12.6416 | 1.08 | — |
| **G2** | 11.27 | 12.6416 | 1.12 | — |
| **G3** | 11.51 | 12.6416 | 1.10 | — |
| **Copper Average** | — | — | 1.10 | 0.02 |
| **Total Flux Wire Average** | — | — | 1.19 | 0.08 |

### *3.3.3 Capsule Peak Fluence Calculations and Lead Factor Determinations*

Table 3-8 provides the best-estimate fast neutron fluence and lead factors determined for each of the OEM surveillance capsules installed in the Peach Bottom Unit 2 reactor. The fluence and lead factor for the 30° capsule is reported at the time it was removed from the reactor. Fluence and lead factors are given for the 300° capsule remaining in the reactor at assumed exposures of EOC 22 and 70 EFPY. Note that the 120° and 300° capsules are symmetrical locations and therefore are predicted to have the same fluence and lead factor.

**Table 3-8**
**Best-Estimate Fluence and Lead Factors Determined for the Peach Bottom Unit 2 Surveillance Capsules**

| Evaluated Time Period | Capsule Fluence ($n/cm^2$) | | Peak RPV Fluence ($n/cm^2$) | | Lead Factor[1][2] | | | |
|---|---|---|---|---|---|---|---|---|
| | | | | | 30° | | 120°/300° | |
| | 30° | 120°/300° | 0T | 1/4T | 0T | 1/4T | 0T | 1/4T |
| EOC 7 | — | 2.59E+17 | 2.50E+17 | 1.74E+17 | — | — | 1.04 | 1.49 |
| EOC 22 | 9.13E+17 | — | 9.01E+17 | 6.24E+17 | 1.01 | 1.46 | — | — |
| 70 EFPY | — | 2.02E+18 | 2.04E+18 | 1.42E+18 | — | — | 0.99 | 1.42 |

1. The lead factor is defined as the ratio of the fast neutron fluence at the center of the surveillance capsule to the peak fast neutron fluence at the base metal inner surface (0T) of the RPV.
2. A second lead factor is provided using the peak damage fluence at the 1/4T depth of the RPV wall.

It is observed in Table 3-8 that the capsule fluence is nearly identical to the RPV peak fluence. The calculated-to-measured activation comparisons for the OEM surveillance capsule presented in the previous sections show no discernable bias in the computational fluence method. Therefore, the best-estimate fluence reported for each capsule in Table 3-8 is the unbiased fast neutron fluence computed by the fluence methodology. This is discussed further in Section 3.4.

## 3.4 Capsule Fluence Uncertainty Analysis

This section presents the combined uncertainty analysis and the determination of bias for the Peach Bottom Unit 2 OEM capsule fluence evaluation. The combined uncertainty is comprised of two components. One component is the uncertainty factors developed from plant-specific measurements and the other is an analytic uncertainty factor. When combined, these components provide a basis for determining the combined uncertainty ($1\sigma$) and bias in the computed RPV fluence.

The requirements for determining the combined uncertainty and bias for light water reactor pressure vessel fluence evaluations are provided in Regulatory Guide 1.190 [14]. The approach for determining combined uncertainty and bias for reactor component fluence is demonstrated in Reference 19.

For capsule fluence evaluations, two uncertainty factors are considered: comparison factors and uncertainty introduced by the measurement process. After analysis of these factors, it was determined that the combined uncertainty for Peach Bottom Unit 2 30° capsule fluence was 10.18%, and that no adjustment for bias was required for the calculated capsule fast neutron fluence presented in Section 3.3 of this report.

The following subsections describe the comparison uncertainties, the determination of the analytic uncertainty, and the determination of the overall combined uncertainty and bias for the Peach Bottom Unit 2 capsule fluence evaluation.

### *3.4.1 Comparison Uncertainty*

Comparison uncertainty factors are determined by comparing calculated activities with activity measurements. For capsule fluence evaluations, two comparison uncertainty factors are considered: plant-specific comparison factors and benchmark comparison factors. Comparison uncertainty factors based upon measurements also involve the combination of two components: the calculated-to-measured (C/M) activity ratio and a measurement uncertainty.

#### 3.4.1.1 Operating Reactor Comparison Uncertainty

TransWare has evaluated activation measurements for several BWR plants ranging from BWR/2-class plants to BWR/6-class plants. Each class of BWRs can have one or several variations of reactor core configurations, each having different radial diameters for the core shroud, reactor pressure vessel, and biological shield components. In addition, each can have different placements of the jet pumps and surveillance capsules in the reactor vessels.

The Peach Bottom Unit 2 reactor is a BWR/4 class design. A total of 233 plant-specific dosimetry measurements have been evaluated for BWR/4-class plants using the RAMA Fluence Methodology. The overall C/M and standard deviation for the BWR/4-class plant measurements is determined to be an unbiased $1.03 \pm 0.12$. Of the 233 measurements, fifteen samples were taken from Peach Bottom Unit 2. A total of 628 credible activation measurement comparisons have been previously performed for a broad spectrum of BWR configurations and designs using the RAMA Fluence Methodology. The overall comparison ratio for all BWR class plants evaluated as of the date of this report is $1.00 \pm 0.10$. Note that only the BWR/4-class plant measurement data is utilized in this analysis to determine the operating reactor uncertainty factor.

#### 3.4.1.2 Benchmark Comparison Uncertainty

The comparison uncertainty is based on a set of industry standard simulation benchmark comparisons. In accordance with the guidelines provided in Regulatory Guide 1.190, it is appropriate to include comparisons of vessel simulation benchmark measurements in the overall fluence uncertainty evaluation. Two vessel simulation benchmarks are evaluated: the Pool Critical Assembly (PCA) and VENUS-3 experimental benchmarks.

The PCA experimental benchmark includes 27 activation measurements at the mid-plane elevation in various simulated reactor components. The VENUS-3 experimental benchmark includes 386 activation measurements at a range of elevations in various simulated reactor components Table 3-9 summarizes the calculated-to-measurement (C/M) results determined for these vessel simulation benchmarks.

**Table 3-9**
**Summary of Comparisons to Vessel Simulation Benchmark Measurements**

| Benchmark | Number of Measurements | Average Calculated-to-Measured (C/M) | St. Dev. (1σ) |
|---|---|---|---|
| **Pool Critical Assembly** | 27 | 0.99 | ±0.05 |
| **VENUS-3** | 386 | 1.03 | ±0.05 |
| **Total Simulated Vessel Comparisons** | **413** | **1.03** | **±0.05** |

### 3.4.2 Analytic Uncertainty

The calculational models used for fluence analyses are comprised of numerous analytical parameters that have associated uncertainties in their values. The uncertainty in these parameters needs to be tested for its contribution to the overall fluence uncertainty.

The uncertainty values for the geometry parameters are based upon uncertainties in the dimensional data used to construct the plant geometry model. The uncertainty values for the material parameters are based upon uncertainties in the material densities for the water and nuclear fuel materials and the compositional makeup of typical steel materials.

The uncertainty values for the fission source parameters are based upon uncertainties in the fuel exposure and power factors for the fuel assemblies loaded on the core periphery. The transport method used in the fluence analysis employs a fission source calculation that accounts for the relative contributions of the uranium and plutonium fissile isotopes in the fuel and the relative power density of the fuel in the reactor. Both fission source parameters are derived directly from information calculated by three-dimensional core simulator codes. The uncertainty values for the nuclear cross-section parameters are based upon uncertainties in the number densities for the predominant nuclides that make up the reactor materials.

The uncertainty parameters for the fluence model inputs are based upon geometry meshing and numerical integration parameters used in the neutron flux transport calculation. Several mesh size and numerical integration parameter sensitivity cases are run to determine the optimum values for the transport calculation and to determine their corresponding impact on the analytic uncertainty.

### 3.4.3 Combined Uncertainty

The combined uncertainty for the reactor pressure vessel fluence evaluation is determined with a weighting function that combines the analytic, plant-specific comparison, and benchmark comparison uncertainty factors. Table 3-10 shows that the combined uncertainty ($1\sigma$) determined for the Peach Bottom Unit 2 30-degree capsule is 10.18% for neutron energy exceeding 1.0 MeV and contains the uncertainty results for the other capsules.

It is shown in Table 3-10 that the combined uncertainty is well below the 20% uncertainty limit specified in Regulatory Guide 1.190. In accordance with Regulatory Guide 1.190, there is no discernable bias in the computed RPV fluence. Therefore, no adjustment to the calculated capsule fast neutron fluence that is presented in Section 3.3. is required.

**Table 3-10**
**Peach Bottom Unit 2 Surveillance Capsule Combined Uncertainty for Energy >1.0 MeV**

| Capsule | Time of Removal | Accumulated Exposure (EFPY) | Combined Bias[1] | Combined Uncertainty ($1\sigma$) |
|---|---|---|---|---|
| 30° | EOC 7 | 7.5 | 0.0% | 10.18% |
| 120° | EOC 22 | 33.6 | 0.0% | 10.17% |

1. The bias terms are less than their constituent uncertainty values, concluding that no statistically-significant bias exists.

# 4
# CHARPY TEST DATA

## 4.1 Charpy Test Procedure

Charpy impact tests were conducted in accordance with ASTM Standards E185-82 [3] and E23-02 [9]. The 1982 version of E185 has been reviewed and approved by NRC for surveillance capsule testing applications. This standard references ASTM E23. The tests were conducted using a Tinius Olsen Testing Machine Company, Inc. Model 84 impact test machine with a 300 ft-lb (406.75 J) energy capacity. The Model 84 is equipped with a dial gage as well as the MPM optical encoder system for accurate absorbed energy measurement. The machine is also equipped with an instrumented striker, so a total of three independent measurements of the absorbed energy were made for every test. In all cases, the optical encoder measured energy was reported as the impact energy. The optical encoder energy is much more accurate than the analog dial. The optical encoder can resolve the energy to within 0.04 ft-lbs (0.054 J), whereas, for the dial, the resolution is around 0.25 ft-lbs (0.34 J). The impact energy was corrected for windage and friction for each test performed. The velocity of the striker at impact was nominally 18 ft/s (5.49 m/s). The MPM encoder system measures the exact impact velocity for every test. Calibration of the machine was verified as specified in ASTM E23, and verification specimens were obtained from the National Institute for Standards and Technology (NIST) and tested in accordance with the standard.

The ASTM E23 procedure for specimen temperature control using an in-situ heating and cooling system was followed. The advantage of using the MPM in-situ heating/cooling technology is that each specimen is thermally conditioned right up to the instant of impact. Thermal losses associated with liquid bath systems, such as those resulting from transfer of a specimen from a liquid bath to the test machine, are completely eliminated. Each specimen was held at the desired test temperature for at least 5 minutes prior to testing, and the fracture process zone temperature was held to within ± 1.8°F (± 1°C) up to the instant of strike. Precision calibrated tongs were used for specimen centering on the test machine.

Lateral expansion (LE) was determined from measurements made with a lateral expansion gage. The lateral expansion gage was calibrated using precision gage blocks which are traceable to NIST. The percentage of shear fracture area was determined by integrating the ductile and brittle fracture areas using the MPM Digital Optical Comparator (DOC) image analysis system. As shown in Figure 4-1, each fracture surface image is captured, outlined to delineate the brittle area, and outlined to define the outer ductile fracture region. The DOC software then performs a pixel area integration and automatically calculates the shear fracture area. This method for shear area determination is the most accurate method given in ASTM E23, and is far superior to the commonly used photograph comparison method.

The number of Charpy specimens for measurement of the transition region and upper shelf was limited. Therefore, the choice of test temperatures was very important. Prior to testing, the Charpy energy-temperature curve was predicted using embrittlement models and previous data. The first test was then conducted near the middle of the transition region, and test temperature decisions were then made based on the test results. Overall, the goal was to perform two or three tests on the upper shelf, and to use the remaining specimens to characterize the 30 ft-lb (41 J) index. This approach was successful, and the transition region and upper shelf energy are well defined.

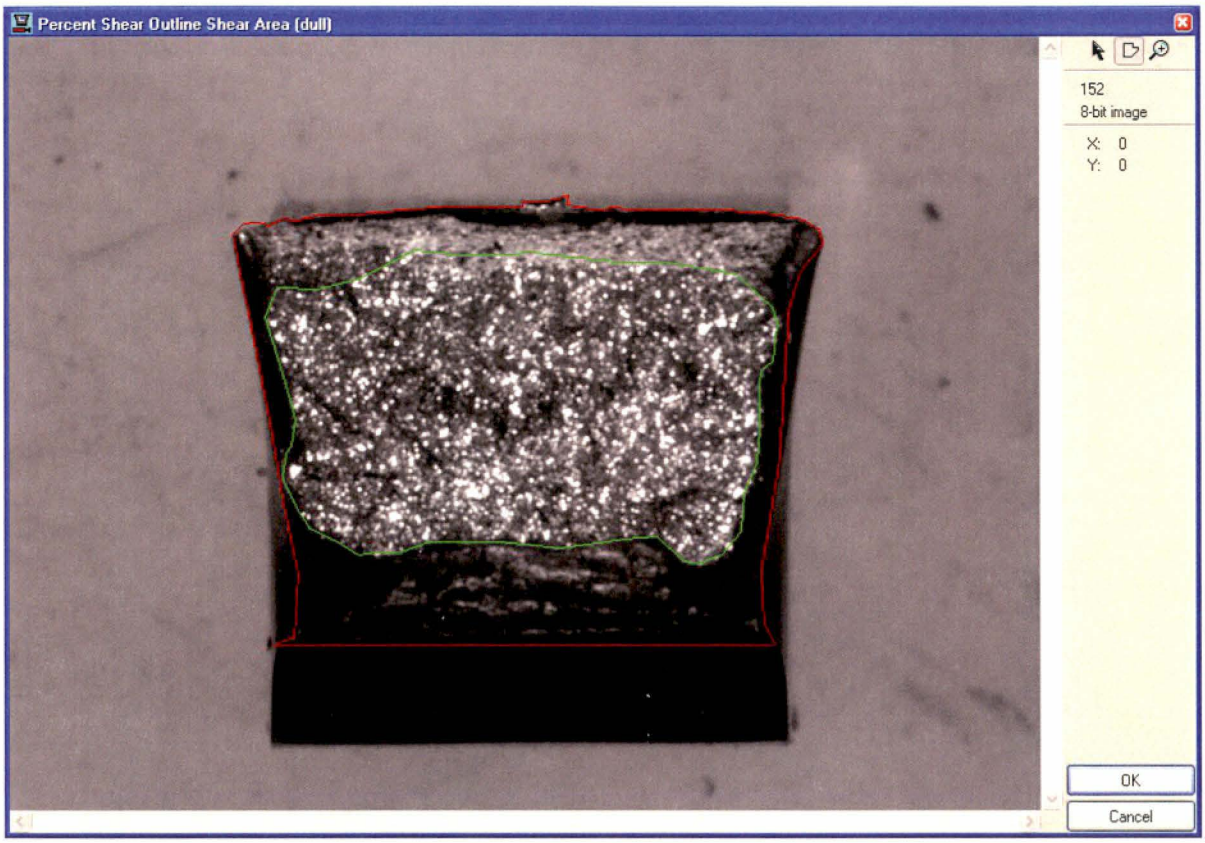


First, the Brittle Fracture Area is Outlined (within green line). Next, the Outer Ductile Fracture Area is Outlined (within red line). Finally, the Software Integrates the Areas and Calculates the Percent Shear Fracture Area.

**Figure 4-1**
**Illustration of Digital Optical Comparator Measurement of Shear Fracture Area**

## 4.2 Charpy Test Data for the 30° Capsule

A total of twelve irradiated base, twelve irradiated weld, and twelve irradiated HAZ metal specimens were tested over the transition region temperature range and on the upper shelf. The data are summarized in Tables 4-1 through 4-3. In addition to the energy absorbed by the specimen during impact, the measured lateral expansion values and the percentage shear fracture area for each test specimen are listed in the tables. The Charpy energy was acquired from the optical encoder signal and has been corrected for windage and friction in accordance with ASTM E23. The impact energy is the energy required to initiate and propagate a crack in the Charpy

specimen. The optical encoder and the dial cannot correct for tossing energy or losses in the test machine, and therefore this small amount of additional energy, if present, may be included in the data for some tests. The instrumented striker energy does not include tossing energy or machine vibration energy since the energy, in this case, is measured only during a few milliseconds of contact between the striker and specimen. Based on comparison between the instrumented striker energy and the optical encoder energy, it has been shown that the tossing energy, and other losses, are small for most tests.

The lateral expansion is a measure of the transverse plastic deformation produced by the contact edge of the striker during the impact event. Lateral expansion is determined by measuring the maximum change of specimen thickness along the sides of the specimen. Lateral expansion is a measure of the ductility of the specimen. The nuclear industry tracks the embrittlement shift using the 35 mil (0.89 mm) lateral expansion index. In accordance with ASTM E23, the lateral expansion for some specimens, which could not be broken by hand after the impact test, should not be reported as broken since the lateral expansion of the unbroken specimen is less than that for the broken specimen. Therefore, when these conditions exist, the value listed is the unbroken measurement and a footnote is included to identify these specimens. All of the 30° capsule specimens that did not separate during the test could be broken by hand under the ASTM E23 requirements.

The percentage of shear fracture area is a direct quantification of the transition in the fracture modes as the temperature increases. All metals with a body centered cubic lattice structure, such as ferritic pressure vessel materials, undergo a transition in fracture modes. At low test temperatures, a crack propagates in a brittle manner and cleaves across the grains. As the temperature increases, the percentage of shear (or ductile) fracture increases. This temperature range is referred to as the transition region and the fracture process is mixed mode. As the temperature increases further, the fracture process is eventually completely ductile (i.e., no brittle component) and this temperature range is referred to as the upper shelf region.

**Table 4-1**
**Irradiated Charpy V-Notch Impact Test Results for Surveillance Base Metal Specimens (Heat C2761-2) from the Peach Bottom Unit 2 30° Surveillance Capsule**

| Base Irradiated: Heat C2761-2, Longitudinal, 30° Capsule | | | | | | | |
|---|---|---|---|---|---|---|---|
| Specimen | Test Temperature | | Impact Energy | | Lateral Expansion | | Percent Shear |
| ID | °F | (°C) | ft-lb | (J) | mils | (mm) | (%) |
| 761 | -48.3 | (-44.6) | 9.68 | (13.12) | 7.8 | (0.20) | 6.3 |
| 775 | -25.0 | (-31.7) | 29.38 | (39.83) | 24.2 | (0.61) | 11.0 |
| 76L | -0.9 | (-18.3) | 20.32 | (27.55) | 17 | (0.43) | 17.6 |
| 77C | 14.9 | (-9.5) | 38.1 | (51.66) | 32.2 | (0.82) | 23.2 |
| 76P | 33.8 | (1.0) | 47.76 | (64.75) | 41.8 | (1.06) | 30.5 |
| 757 | 68.5 | (20.3) | 67.8[a] | (91.92) | 56 | (1.42) | 41.6 |
| 76T | 96.6 | (35.9) | 106.51 | (144.41) | 73.3 | (1.86) | 66.5 |
| 76Y | 123.1 | (50.6) | 121.26 | (164.40) | 74.2 | (1.88) | 83.0 |
| 75E | 151.9 | (66.6) | 112.44 | (152.45) | 81.7 | (2.08) | 90.2 |
| 75U | 302.5 | (150.3) | 140.05 | (189.88) | 92.9 | (2.36) | 100 |
| 774 | 251.8 | (122.1) | 135.85 | (184.19) | 80.4 | (2.04) | 100 |
| 77U | 354.7 | (179.3) | 136.69 | (185.32) | 85.6 | (2.17) | 100 |

[a] For specimen 757, an error occurred when reading the encoder energy so the dial energy was used.

**Table 4-2**
**Irradiated Charpy V-Notch Impact Test Results for Surveillance Weld Metal Specimens (Heat PB2 ESW) from the Peach Bottom Unit 2 30° Surveillance Capsule**

| Weld Irradiated: Heat PB2 ESW, 30° Capsule | | | | | | | |
|---|---|---|---|---|---|---|---|
| Specimen | Test Temperature | | Impact Energy | | Lateral Expansion | | Percent Shear |
| ID | °F | (°C) | ft-lb | (J) | mils | (mm) | (%) |
| 7AJ | -51.5 | (-46.4) | 5.54 | (7.51) | 3.2 | (0.08) | 0.7 |
| 7C5 | -26.9 | (-32.7) | 3.24 | (4.39) | 1.9 | (0.05) | 2.0 |
| 7AK | -1.8 | (-18.8) | 23.37 | (31.69) | 17.7 | (0.45) | 9.1 |
| 7CJ | 21.9 | (-5.6) | 27.76 | (37.64) | 26 | (0.66) | 12.9 |
| 7AP | 37.2 | (2.9) | 41.63 | (56.44) | 34.2 | (0.87) | 19.0 |
| 7A7 | 69.4 | (20.8) | 60.46 | (81.97) | 53.9 | (1.37) | 32.5 |
| 7AY | 111.4 | (44.1) | 84.41 | (114.44) | 53.2 | (1.35) | 57.5 |
| 7B5 | 156.0 | (68.9) | 100.17 | (135.81) | 67.8 | (1.72) | 78.8 |
| 7AA | 203.4 | (95.2) | 108.76 | (147.46) | 86.3 | (2.19) | 94.9 |
| 7BD | 248.9 | (120.5) | 113.99 | (154.55) | 69.8 | (1.77) | 99.9 |
| 7AC | 299.7 | (148.7) | 117.98 | (159.96) | 84.3 | (2.14) | 100 |
| 7CK | 351.7 | (177.6) | 120.81 | (163.79) | 78.1 | (1.98) | 100 |

**Table 4-3**
**Irradiated Charpy V-Notch Impact Test Results for Surveillance HAZ Metal Specimens from the Peach Bottom Unit 2 30° Surveillance Capsule**

| HAZ Irradiated: 120° Capsule | | | | | | | |
|---|---|---|---|---|---|---|---|
| Specimen | Test Temperature | | Impact Energy | | Lateral Expansion | | Percent Shear |
| ID | °F | (°C) | ft-lb | (J) | mils | (mm) | (%) |
| 7DE | -50.8 | (-46.0) | 11.86 | (16.08) | 11.3 | (0.29) | 7.9 |
| 7E5 | 19.2 | (-7.1) | 28.9 | (39.18) | 25 | (0.64) | 14.0 |
| 7DJ | -1.3 | (-18.5) | 18.82 | (25.52) | 19.6 | (0.50) | 22.9 |
| 7EK | 29.5 | (-1.4) | 47.09 | (63.84) | 39.5 | (1.00) | 26.0 |
| 7CT | 69.3 | (20.7) | 56.96 | (77.23) | 46.5 | (1.18) | 43.6 |
| 7J6 | 51.8 | (11.0) | 38.15 | (51.72) | 32.5 | (0.83) | 45.4 |
| 7DY | 38.1 | (3.4) | 106.64 | (144.58) | 75.3 | (1.91) | 59.3 |
| 7E1 | 112.8 | (44.9) | 148.2 | (200.93) | 84.6 | (2.15) | 89.3 |
| 7J7 | 91.8 | (33.2) | 143.04 | (193.93) | 84.7 | (2.15) | 90.5 |
| 7DA | 202.1 | (94.5) | 119.26 | (161.69) | 90.1 | (2.29) | 100 |
| 7DC | 300.7 | (149.3) | 113.67 | (154.11) | 81.8 | (2.08) | 100 |
| 7E3 | 154.4 | (68.0) | 128.92 | (174.79) | 81.2 | (2.06) | 100 |

# 5
# CHARPY TEST RESULTS

## 5.1 Analysis of Impact Test Results

For analysis of the Charpy test data, the BWRVIP ISP has selected the hyperbolic tangent (tanh) function as the statistical curve-fit tool to model the transition temperature toughness data. A hyperbolic tangent curve-fitting program named CVGRAPH [10] was used to fit the Charpy V-notch (CVN) energy and lateral expansion data. Analysis methodology (e.g., definition of upper fixed shelf and lower shelf) followed the BWRVIP conventions established for analysis of all ISP data [20]. The impact energy curve-fit from CVGRAPH are provided in Figure 5-1 (plate heat C2761-2) and Figure 5-2 (weld heat PB2 ESW). The lateral expansion curve fits are provided in Figure 5-3 (plate heat C2761-2) and Figure 5-4 (weld heat PB2 ESW). HAZ results are not used in the BWRVIP ISP; thus, the HAZ data were not fit.

For the analysis of Charpy energy test data, lower shelf energy was fixed at 2.5 ft-lbs (3.4 J). Upper shelf energy was fixed at the average of all test energies exhibiting shear greater than or equal to 95%, consistent with ASTM Standard E185-82 [3]. For analysis of the lateral expansion test data, the lower shelf was fixed at 1.0 mils; the fixed upper shelf was defined as the average of the lateral expansion test data points exhibiting shear greater than or equal to 95%, consistent with the approach used for upper shelf energy.

## 5.2 Irradiated Versus Unirradiated CVN Properties

Table 5-1 summarizes the $T_{30}$ [30 ft-lb (41 J) Transition Temperature], $T_{35mil}$ [35 mil (0.89 mm) Lateral Expansion Temperature], $T_{50}$ [50 ft-lb (68 J) Transition Temperature], and Upper Shelf Energy for the unirradiated and irradiated materials and shows the change (shift) from baseline values. The unirradiated values of $T_{30}$ and $T_{50}$ were taken from the CVGRAPH fits provided in Figures 2-5 and 2-6; the unirradiated values of $T_{35mil}$ were taken from the CVGRAPH fits provided in Figures 2-7 and 2-8. The irradiated values are from the index temperatures determined in Figures 5-1 and 5-2 for impact energy and Figures 5-3 and 5-4 for lateral expansion.

Table 5-2 provides a comparison of the measured $T_{30}$ shift to the predicted shift for plate heat C2761-2 and weld heat PB2 ESW. Predicted shift is based on the formula provided in Regulatory Position 1.1 of Reg. Guide 1.99, Rev. 2 [6] as shown in Note 3 to Table 5-2. The fluence was input as $9.13 \times 10^{17}$ n/cm$^2$, as reported in Table 3-8 for the 30° surveillance capsule. The measured shift for the surveillance plate and weld are less than the value expected (e.g., the measured shift is less than predicted shift + margin).

Measured percent decrease in USE is presented in Table 5-3 and compared to the percent decrease predicted by Regulatory Position 1.2 and Figure 2 of Reg. Guide 1.99, Rev. 2. The measured percent decrease in USE for the surveillance plate and weld are less than the predicted percent decrease.

## Irradiated Plate Heat C2761-2 (PB2-30)

CVGraph 6.02: Hyperbolic Tangent Curve Printed on 3/24/2020 6:24 AM

**A = 70.02 B = 67.52 C = 82.83 T0 = 60.64 D = 0.00**

Correlation Coefficient = 0.990

Equation is A + B * [Tanh((T-T0)/(C+DT))]

Upper Shelf Energy = 137.53 (Fixed) Lower Shelf Energy = 2.50 (Fixed)

Temp@30 ft-lbs= 4.20° F Temp@35 ft-lbs= 13.10° F Temp@50 ft-lbs= 35.40° F

Plant: **Peach Bottom 2** Material: **SA302BM** Heat: **C2761-2**
Orientation: **LT** Capsule: **30 DEG** Fluence: **n/a**

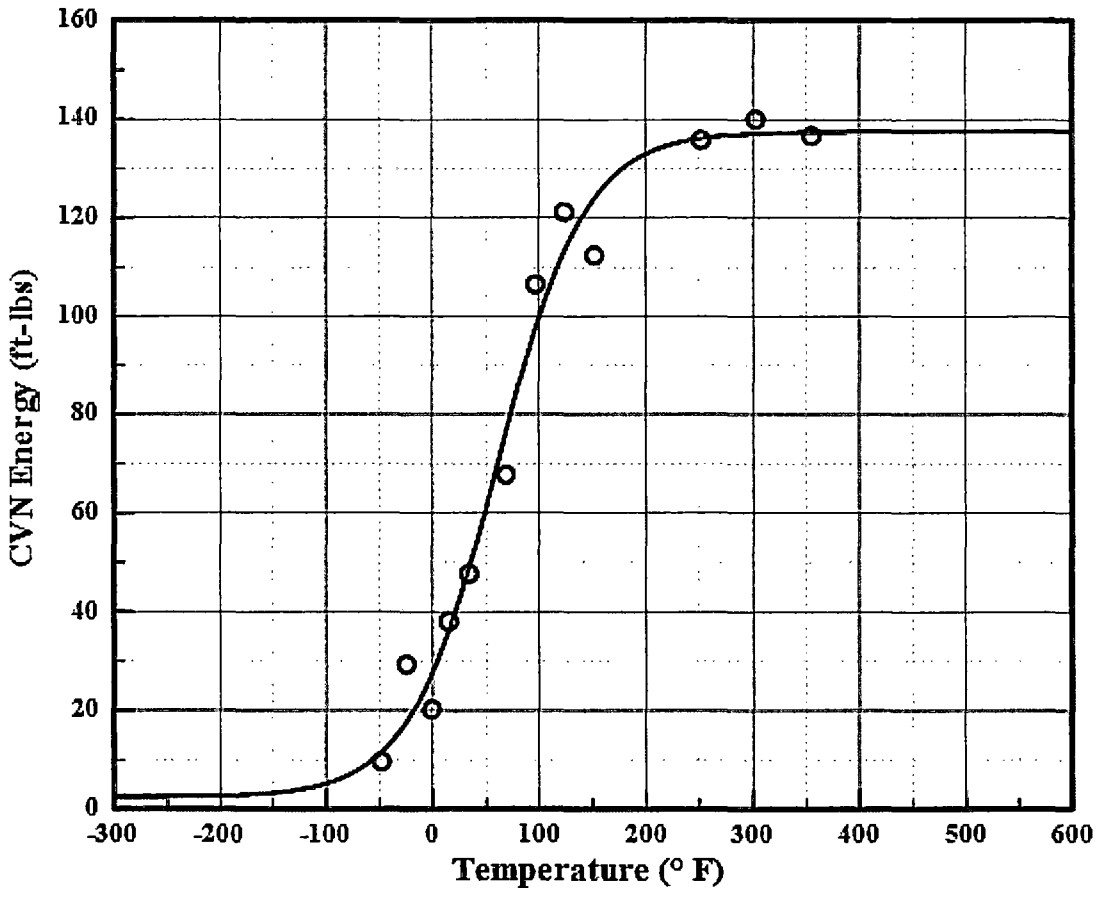


CVGraph 6.02 03/24/2020 Page 1/2

**Figure 5-1**
**Irradiated Plate Heat C2761-2 Charpy Energy Plot (Peach Bottom Unit 2 30° Capsule) (LT)**

Plant: **Peach Bottom 2** Material: **SA302BM** Heat: **C2761-2**
Orientation: **LT** Capsule: **30 DEG** Fluence: **n/a**

# Irradiated Plate Heat C2761-2 (PB2-30)

## Charpy V-Notch Data

| Temperature (° F) | Input CVN | Computed CVN | Differential |
|---|---|---|---|
| -48 | 9.7 | 11.6 | -1.89 |
| -25 | 29.4 | 17.7 | 11.72 |
| -1 | 20.3 | 27.4 | -7.10 |
| 15 | 38.1 | 36.1 | 1.99 |
| 34 | 47.8 | 48.9 | -1.11 |
| 69 | 67.8 | 76.4 | -8.60 |
| 97 | 106.5 | 97.6 | 8.90 |
| 123 | 121.3 | 113.1 | 8.20 |
| 152 | 112.4 | 124.1 | -11.66 |
| 303 | 140.1 | 137.1 | 2.91 |
| 252 | 135.9 | 136.2 | -0.36 |
| 355 | 136.7 | 137.4 | -0.73 |

CVGraph 6.02 03/24/2020 Page 2/2

**Figure 5-1 (continued)**
**Irradiated Plate Heat C2761-2 Charpy Energy Plot (Peach Bottom Unit 2 30° Capsule) (LT)**

## Irradiated Weld Heat PB2 ESW (PB2-30)

CVGraph 6.02: Hyperbolic Tangent Curve Printed on 3/24/2020 6:32 AM

**A = 58.95 B = 56.45 C = 82.41 T0 = 69.56 D = 0.00**

Correlation Coefficient = 0.996

Equation is A + B * [Tanh((T-T0)/(C+DT))]

Upper Shelf Energy = 115.39 (Fixed) Lower Shelf Energy = 2.50 (Fixed)

Temp@30 ft-lbs= 22.90° F Temp@35 ft-lbs= 32.30° F Temp@50 ft-lbs= 56.40° F

Plant: **Peach Bottom 2** Material: **ESW** Heat: **PB2 ESW**

Orientation: **NA** Capsule: **30 DEG** Fluence: **n/a**

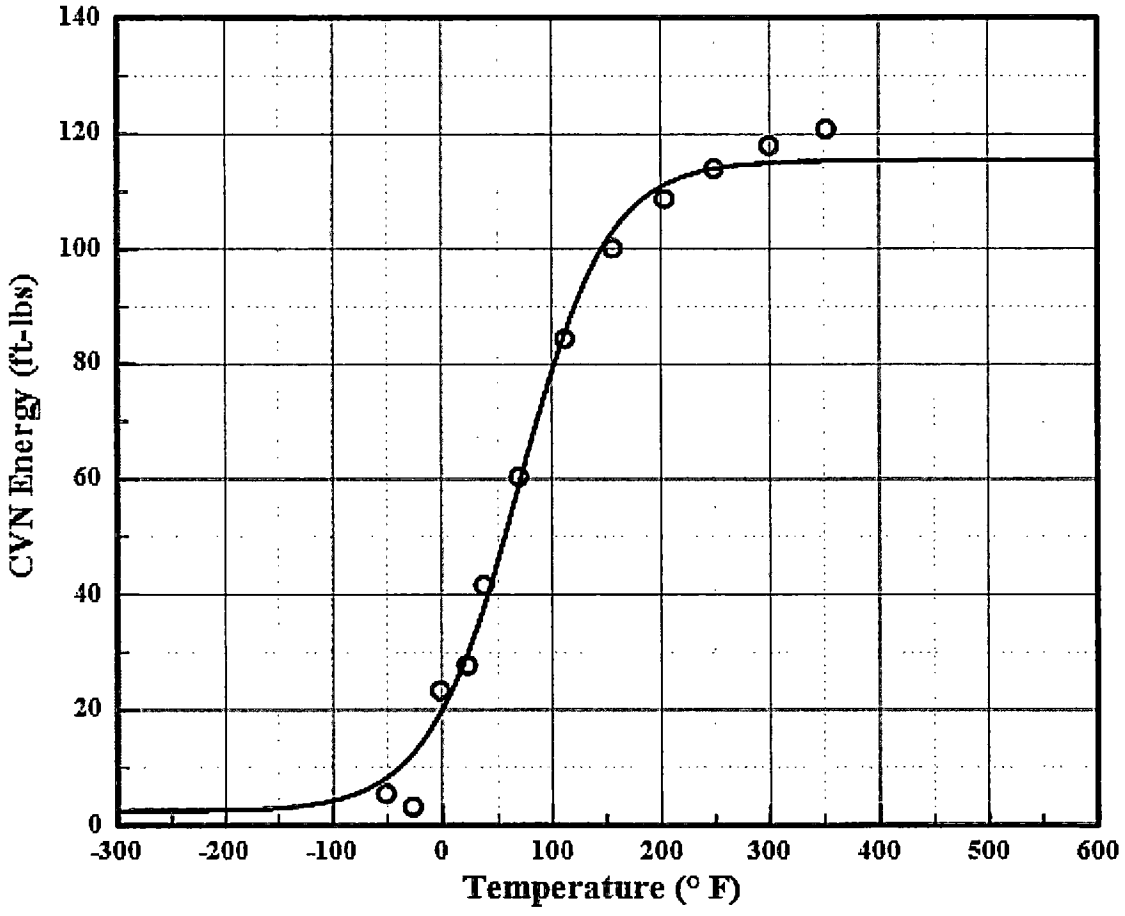


CVGraph 6.02 03/24/2020 Page 1/2

**Figure 5-2**
**Irradiated Weld Heat PB2 ESW Charpy Energy Plot (Peach Bottom Unit 2 30° Capsule)**

Plant: **Peach Bottom 2** Material: **ESW** Heat: **PB2 ESW**
Orientation: **NA** Capsule: **30 DEG** Fluence: **n/a**

# Irradiated Weld Heat PB2 ESW (PB2-30)

## Charpy V-Notch Data

| Temperature (° F) | Input CVN | Computed CVN | Differential |
|---|---|---|---|
| -52 | 5.5 | 8.2 | -2.64 |
| -27 | 3.2 | 12.4 | -9.17 |
| -2 | 23.4 | 19.5 | 3.90 |
| 22 | 27.8 | 29.5 | -1.75 |
| 37 | 41.6 | 37.9 | 3.78 |
| 69 | 60.5 | 58.8 | 1.62 |
| 111 | 84.4 | 85.4 | -0.96 |
| 156 | 100.2 | 103.1 | -2.88 |
| 203 | 108.8 | 111.2 | -2.41 |
| 249 | 114.0 | 114.0 | 0.03 |
| 300 | 118.0 | 115.0 | 3.01 |
| 352 | 120.8 | 115.3 | 5.54 |

CVGraph 6.02 03/24/2020 Page 2/2

**Figure 5-2 (continued)**
**Irradiated Plate Heat PB2 ESW Charpy Energy Plot (Peach Bottom Unit 2 30° Capsule)**

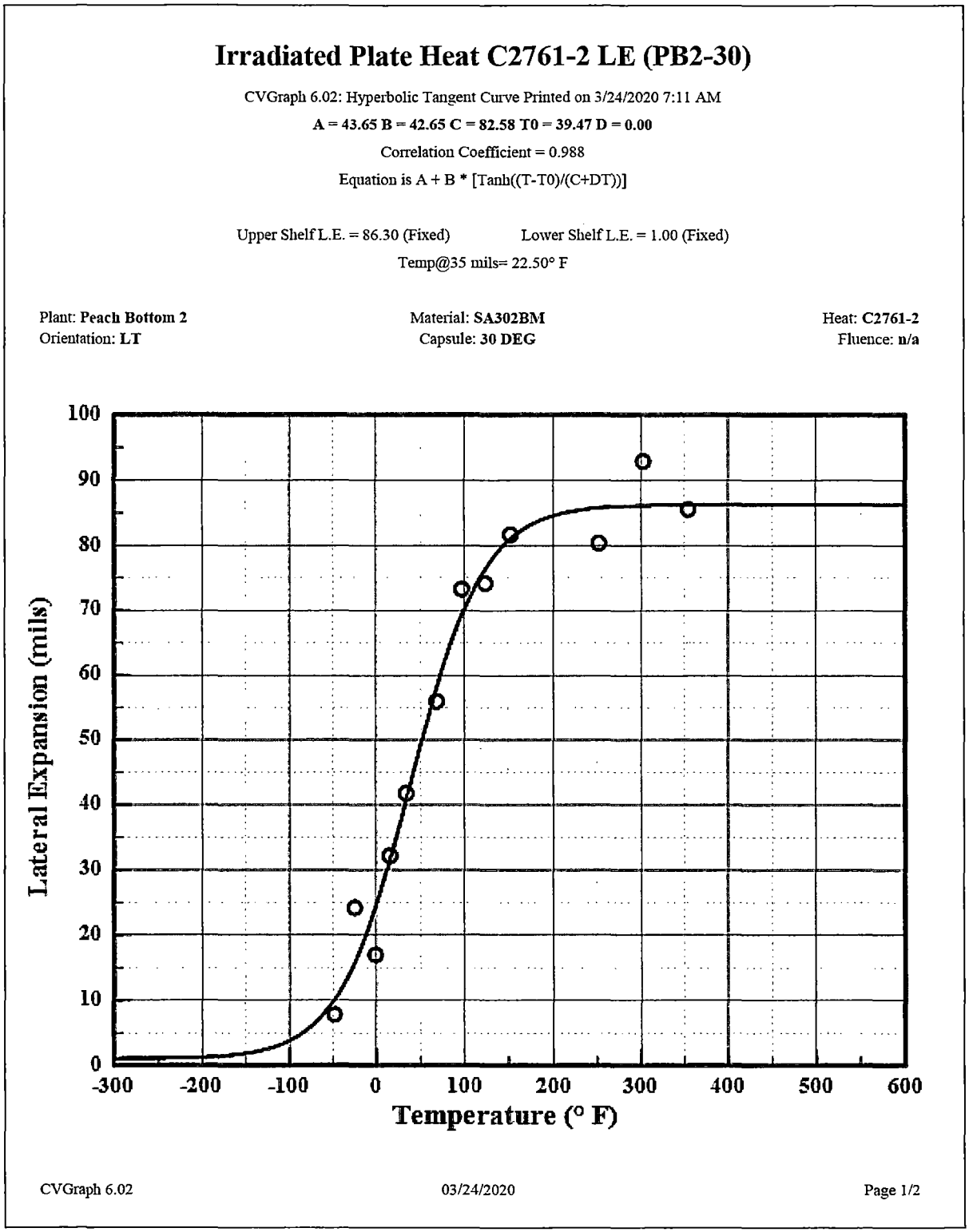


**Figure 5-3**
**Irradiated Plate Heat C2761-2 Lateral Expansion Plot (Peach Bottom Unit 2 30° Capsule) (LT)**

Plant: **Peach Bottom 2** Material: **SA302BM** Heat: **C2761-2**
Orientation: **LT** Capsule: **30 DEG** Fluence: **n/a**

# Irradiated Plate Heat C2761-2 LE (PB2-30)

## Charpy V-Notch Data

| Temperature (° F) | Input L. E. | Computed L. E. | Differential |
|---|---|---|---|
| -48 | 7.8 | 10.1 | -2.29 |
| -25 | 24.2 | 15.8 | 8.41 |
| -1 | 17.0 | 24.3 | -7.32 |
| 15 | 32.2 | 31.3 | 0.88 |
| 34 | 41.8 | 40.7 | 1.08 |
| 69 | 56.0 | 58.1 | -2.05 |
| 97 | 73.3 | 69.2 | 4.10 |
| 123 | 74.2 | 76.4 | -2.16 |
| 152 | 81.7 | 81.0 | 0.66 |
| 303 | 92.9 | 86.2 | 6.75 |
| 252 | 80.4 | 85.8 | -5.40 |
| 355 | 85.6 | 86.3 | -0.66 |

CVGraph 6.02 03/24/2020 Page 2/2

**Figure 5-3 (continued)**
**Irradiated Plate Heat C2761-2 Lateral Expansion Plot (Peach Bottom Unit 2 30° Capsule) (LT)**

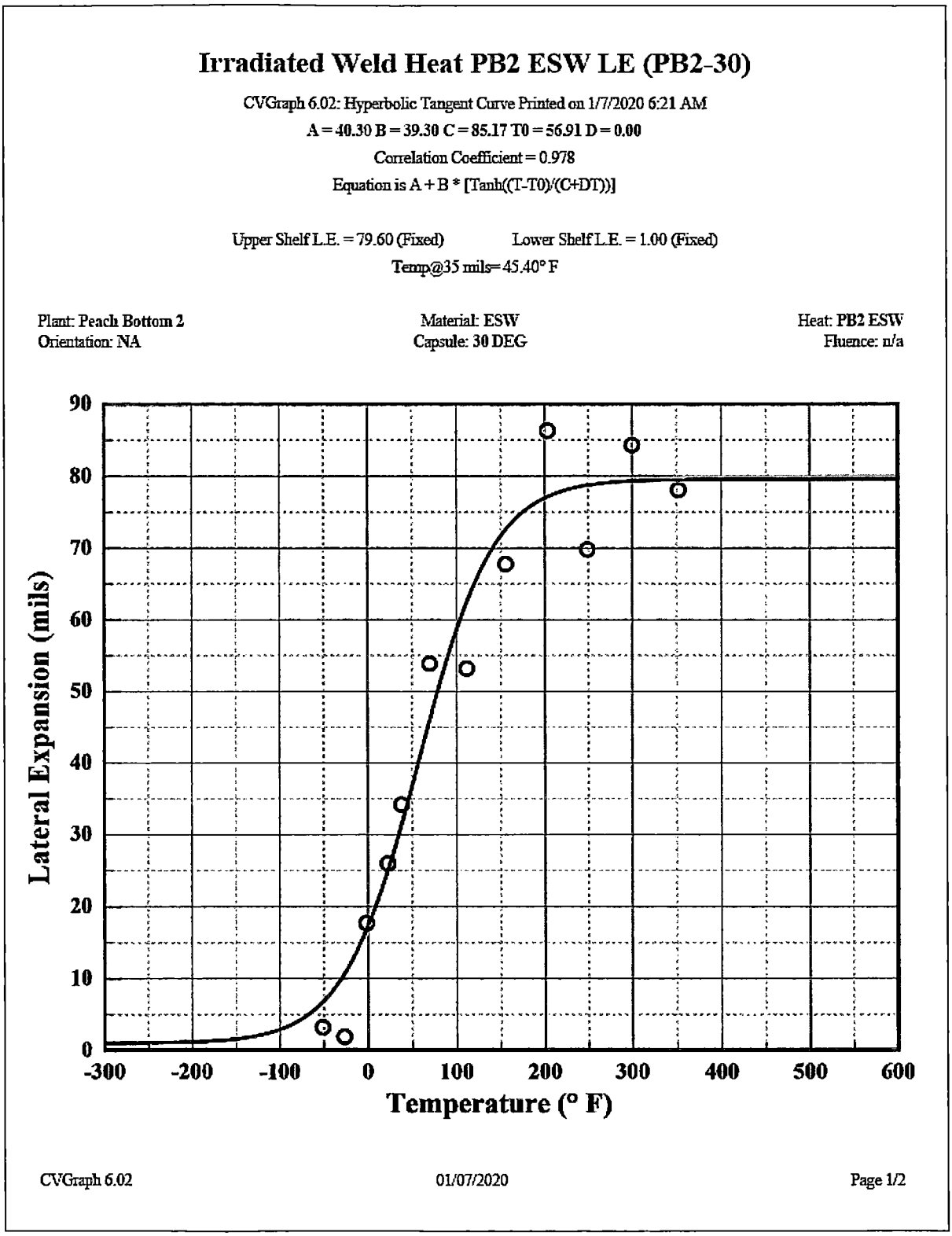


**Figure 5-4**
**Irradiated Weld Heat PB2 ESW Lateral Expansion Plot (Peach Bottom Unit 2 30° Capsule)**

Plant: **Peach Bottom 2** Material: **ESW** Heat: **PB2 ESW**
Orientation: **NA** Capsule: **30 DEG** Fluence: **n/a**

# Irradiated Weld Heat PB2 ESW LE (PB2-30)

## Charpy V-Notch Data

| Temperature (° F) | Input L. E. | Computed L. E. | Differential |
|---|---|---|---|
| -52 | 3.2 | 6.7 | -3.51 |
| -27 | 1.9 | 10.6 | -8.74 |
| -2 | 17.7 | 16.8 | 0.88 |
| 22 | 26.0 | 25.0 | 1.00 |
| 37 | 34.2 | 31.4 | 2.84 |
| 69 | 53.9 | 46.0 | 7.88 |
| 111 | 53.2 | 62.5 | -9.30 |
| 156 | 67.8 | 72.6 | -4.81 |
| 203 | 86.3 | 77.2 | 9.14 |
| 249 | 69.8 | 78.7 | -8.94 |
| 300 | 84.3 | 79.3 | 4.96 |
| 352 | 78.1 | 79.5 | -1.42 |

CVGraph 6.02 01/07/2020 Page 2/2

**Figure 5-4 (continued)**
**Irradiated Weld Heat PB2 ESW Lateral Expansion Plot (Peach Bottom Unit 2 30° Capsule)**

**Table 5-1**
**Effect of Irradiation (E>1.0 MeV) on the Notch Toughness Properties**

| Material Identity | $T_{30}$, 30 ft-lb (40.7 J) Transition Temperature | | | $T_{50}$, 50 ft-lb (67.8 J) Transition Temperature | | | $T_{35mil}$, 35 mil (0.89 mm) Lateral Expansion Temperature | | | CVN Upper Shelf Energy (USE) | | |
|---|---|---|---|---|---|---|---|---|---|---|---|---|
| | Unirrad °F (°C) | Irradiated °F (°C) | $\Delta T_{30}$ °F (°C) | Unirrad °F (°C) | Irradiated °F (°C) | $\Delta T_{50}$ °F (°C) | Unirrad °F (°C) | Irradiated °F (°C) | $\Delta T_{35mil}$ °F (°C) | Unirrad ft-lb (J) | Irradiated ft-lb (J) | Change ft-lb (J) |
| C2761-2 (LT orientation) | -9.6 (-23.1) | 4.2 (-15.4) | 13.8 (7.7) | 12.3 (-10.9) | 35.4 (1.9) | 23.1 (12.8) | 6.4 (-14.2) | 22.5 (-5.3) | 16.1 (8.9) | 127.2 (172.5) | 137.5 (186.5) | 10.3 (14.0) |
| PB2 ESW | 3.0 (-16.1) | 22.9 (-5.1) | 19.9 (11.1) | 41.4 (5.2) | 56.4 (13.6) | 15.0 (8.3) | 25.1 (-3.8) | 45.4 (7.4) | 20.3 (11.3) | 110.9 (150.4) | 115.4 (156.4) | 4.5 (6.0) |

**Table 5-2**
**Comparison of Actual Versus Predicted Embrittlement**

| Identity | Material | Fluence (E>1.0 MeV, $x10^{17}$ n/cm$^2$)[1] | Measured Shift[2] °F (°C) | RG 1.99 Rev. 2 Predicted Shift[3] °F (°C) | RG 1.99 Rev. 2 Predicted Shift+Margin[3,4] °F (°C) |
|---|---|---|---|---|---|
| C2761-2 (LT orientation) | Peach Bottom Unit 2 surveillance plate | 9.13 | 13.8 (7.7) | 25.9 (14.4) | 51.9 (28.8) |
| PB2 ESW | Peach Bottom Unit 2 surveillance weld | 9.13 | 19.9 (11.1) | 33.6 (18.7) | 67.2 (37.3) |

1. Fluence value is reported in Table 3-8.
2. The measured shift is taken from Table 5-1.
3. Predicted shift = CF × FF, where CF is a Chemistry Factor taken from the base metal table in USNRC RG 1.99, Rev. 2 [6], based on each material's Cu/Ni content, and FF is Fluence Factor, $f^{0.28-0.10 \log f}$, where f = fluence in units of $10^{19}$ n/cm$^2$ (E > 1.0 MeV) specified.
4. Margin = $2\sqrt{(\sigma_i^2 + \sigma_\Delta^2)}$, where $\sigma_i$ = the standard deviation on initial $RT_{NDT}$ ($\sigma_i$ is taken to be 0°F), and $\sigma_\Delta$ is the standard deviation on $\Delta RT_{NDT}$ (28°F for welds and 17°F for base materials, except that $\sigma_\Delta$ need not exceed 0.50 times the mean value of $\Delta RT_{NDT}$). Thus, margin is defined as 34°F for plate materials and 56°F for weld materials, or margin equals shift (whichever is less), per Reg. Guide 1.99, Rev. 2.

**Table 5-3**
**Percent Decrease in Upper Shelf Energy**

| Identity | Material | Fluence (E>1.0 MeV, $x10^{17}$ $n/cm^2$)[1] | Measured Decrease in USE (%) | Predicted Decrease in USE[2] (%) |
|---|---|---|---|---|
| C2761-2 (LT orientation) | Peach Bottom Unit 2 surveillance plate | 9.13 | --[3] | 10.8 |
| PB2 ESW | Peach Bottom Unit 2 surveillance weld | 9.13 | --[3] | 13.6 |

1. Fluence value is reported in Table 3-8.
2. Based on the equations for Figure 2 of Reg. Guide 1.99, Rev. 2 [6] as provided in Reg. Guide 1.162 [21].
3. Value less than zero.

# 6
# REFERENCES


1. 10 CFR 50, Appendices G (*Fracture Toughness Requirements*) and H (*Reactor Vessel Material Surveillance Program Requirements*), Federal Register, Volume 60, No. 243, dated December 19, 1995.
2. American Society of Mechanical Engineers (ASME) Boiler and Pressure Vessel Code (Code), Section XI, "Rules for In service Inspection of Nuclear Power Plant Components," Nonmandatory Appendix G, Fracture Toughness Criteria for Protection Against Failure.
3. ASTM E185-82, *Standard Practice for Conducting Surveillance Tests for Light-Water Cooled Nuclear Power Reactor Vessels*, E706 (IF), American Society for Testing and Materials, Philadelphia, PA, 1982.
4. *BWRVIP-86, Revision 1-A: BWR Vessel and Internals Project, Updated BWR Integrated Surveillance Program (ISP) Implementation Plan.* EPRI, Palo Alto, CA: 2012. 1025144.
5. 10 CFR 50, Appendix B, "Quality Assurance Criteria for Nuclear Power Plants and Fuel Reprocessing Plants," August 28, 2007.
6. U.S. NRC Regulatory Guide 1.99, Revision 2, "Radiation Embrittlement of Reactor Vessel Materials," Revision 2, May 1988.
7. "Guideline for the Management of Materials Issues," NEI 03-08, Nuclear Energy Institute, Washington, DC, Latest Edition.
8. GE Nuclear Energy, "Peach Bottom Atomic Power Station Unit 2 Vessel Surveillance Materials Testing and Fracture Toughness Analysis," SASR 88-24, DRF B13-01445-1, Rev. 1, December, 1991.
9. ASTM Standard E23, *Standard Test Methods for Notch Bar Impact Testing of Metallic Materials*, ASTM International, West Conshohocken, PA, www.astm.org.
10. CVGRAPH, Hyperbolic Tangent Curve Fitting Program, Developed by ATI Consulting, Version 6.02, April 2014.
11. *BWRVIP-126, Revision 2: BWR Vessel Internals Project, RAMA Fluence Methodology Software, Version 1.20.* EPRI, Palo Alto, CA: 2010. 1020240.
12. *BWRVIP-121-A: BWR Vessel and Internals Project, RAMA Fluence Methodology Procedures Manual*, EPRI, Palo Alto, CA: 2009. 1019052.
13. *BWRVIP-114-A: BWR Vessel and Internals Project, RAMA Fluence Methodology Theory Manual*, EPRI, Palo Alto, CA: 2009. 1019049.
14. U.S. NRC Regulatory Guide 1.190, "Calculational and Dosimetry Methods for Determining Pressure Vessel Neutron Fluence," March 2001.

15. U.S. Nuclear Regulatory Commission. Office of Nuclear Reactor Regulation. *Safety Evaluation Report with Open Items Related to the License Renewal of Seabrook Station.* Docket Number 50-443. Washington, D.C.: Office of Nuclear Reactor Regulation, 2012.

16. J. R. Askew, "A Characteristics Formulation of the Neutron Transport Equation in Complicated Geometries," United Kingdom Atomic Energy Authority, AEEW-M 1108, 1972.

17. "BUGLE-96: Coupled 47 Neutron, 20 Gamma-Ray Group Cross Section Library Derived from ENDF/B-VI for LWR Shielding and Pressure Vessel Dosimetry Applications," RSICC Data Library Collection, DL2C-185, March 1996.

18. "VITAMIN-B6: A Fine-Group Cross Section Library Based on ENDF/B-VI Release 3 for Radiation Transport Applications," RSICC Data Library Collection, DLC-184, December 1996.

19. *BWRVIP-189: BWR Vessel and Internals Project, Evaluation of RAMA Fluence Methodology Calculation Uncertainty*. EPRI, Palo Alto, CA: 2008. 1016938.

20. *BWRVIP-135, Revision 3: BWR Vessel and Internals Project, Integrated Surveillance Program (ISP) Data Source Book and Plant Evaluations*. EPRI, Palo Alto, CA: 2014. 3002003144.

21. U.S. NRC Regulatory Guide 1.162, "Format and Content of Report for Thermal Annealing of Reactor Pressure Vessels," February 1996.

# A
# DOSIMETER ANALYSIS

## A.1 Dosimeter Material Description

The Peach Bottom Unit 2 30° surveillance capsule dosimeter materials are pure metal wires which were located within the surveillance capsule along the ends of the Charpy specimens. The wire types provided for the Peach Bottom Unit 2 surveillance program are iron, nickel, and copper. Each wire is nominally three inches (7.62 cm) long. Further discussion of the dosimeter cleaning and mass measurements follows.

## A.2 Dosimeter Cleaning and Mass Measurement

At the time the surveillance capsule Charpy packets were opened, the dosimeter wires were cleaned in an ultrasonic cleaner in an acetone bath and were wiped with acetone wetted wipes to remove loose contamination. Upon receipt at the radiometric laboratory, the wires were visually inspected under a low magnification optical microscope. There was evidence of oxidation indicating the need for chemical etching and further cleaning. This was accomplished by soaking the Fe wire segments in a 4N solution of hydrochloric acid until the oxidation was etched from the surface. Similarly, the Cu and Ni wires were immersed in a 2N solution of nitric acid. The wires were then rinsed with distilled water, wiped once more with ethanol, and then allowed to dry in air at room temperature. The wires then exhibited a clean, shiny appearance. Figures A-1 through A-9 show low-power magnifications of the dosimetry wires as they were found prior to cleaning, and after cleaning and coiling.

The total mass of each wire was measured using a Mettler Toledo XS105DU analytical digital balance. Table A-1 lists the results of these measurements, as well as the identification assigned to each dosimeter. The dosimeter identifications were assigned as the packet ID containing the dosimeter wire and type of dosimeter material.

As previously mentioned, the wires were tightly coiled for subsequent counting and weighing. Each wire was wrapped around a thin metal rod to form a coil of approximately 0.5 inch (12.7 mm) diameter or less, which yields a good approximation to a point source geometry at the distance the dosimeter wires are placed from the gamma detector. The coiled wire segments were pressed firmly against a hard surface to flatten the coil to yield the best counting geometry.

## A.3 Radiometric Analysis

Radiometric analysis was performed using high resolution gamma emission spectroscopy. In this method, gamma emissions from the dosimeter materials are detected and quantified using solid-state gamma ray detectors and computer-based signal processing and spectrum analysis. The specifications of the gamma ray spectrometer system (GRSS) are listed in Table A-2. The GRSS features a hyper pure germanium (HPGe) detector that is housed in a lead-copper shield to reduce background count rates. Standard background subtraction procedures were used.

GRSS calibration was performed using a National Institute for Standards and Technology (NIST) traceable mixed gamma quasi-point source. The Canberra analysis software provides the capability for energy resolution and efficiency calibration using specified standard source information. Calibration information is stored on magnetic disk for use by the spectrographic analysis software package.

Since detector efficiency depends on the source-detector geometry, a fixed-reproducible geometry must be selected for the gamma spectrographic analysis of the dosimeter materials. For the dosimeter wires, the counting geometry was that of a quasi-point source (coiled wire) placed five inches (12.7 cm) vertically from the top surface of the detector shell. In this way, extended sources up to 0.5 inch (1.27 cm) can be analyzed with a good approximation to a point source. The coiled wires were well within the area needed to approximate a point source geometry. The HPGe detector was calibrated for efficiency using the NIST traceable source. The accuracy of the efficiency calibration was checked using a gamma spectrographic analysis of the NIST traceable mixed gamma source. The isotopes contained in the source emit gamma rays which span the energy response of the detector for the dosimeter materials. These measurements show that the efficiency calibration is providing a valid measurement of source activity. The acceptance criteria for these measurements are that the software must yield a valid isotopic identification, and that the quantified activity of each correctly identified isotope must be within the uncertainty specified in the source certification. Validation of system performance was made prior to starting the counting tasks, and upon completion of all counting work for Hatch Unit 2. The counting system performance was acceptable in each case, indicating that the counting system properties did not change during the course of the counting procedure.

Table A-3 shows the counting schedule established for this work. There was no requirement for order of counting since the dosimeter materials still contained sufficient quantities of activation products to allow accurate radio assay. Counting times were more than sufficient to achieve the desired statistical accuracy for gamma emissions of interest in all cases.

Neutrons interact with the constituent nuclei of the dosimeter materials producing radionuclides in varying amounts depending on total neutron fluence, its energy spectrum, and the nuclear properties of the dosimeter materials. Table A-4 lists the reactions of interest and their resultant radionuclide products for each element contained in the dosimeters. These are threshold reactions involving an n-p or n-$\alpha$ interaction.

Finally, Table A-5 presents the primary results of interest for flux and fluence determination. The specific activity units are in dps/mg, which normalizes the activity to dosimeter mass. The activities are specified for a useful reference date/time, which in this case is the Peach Bottom Unit 2 plant shutdown date and time. This reference date/time was specified as October 15, 2018, at 12:30:00 AM eastern standard time.

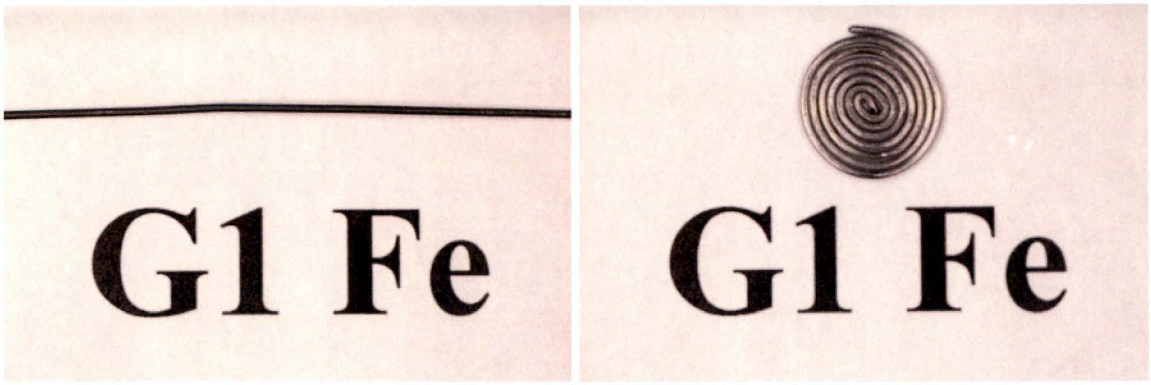


**Figure A-1**
**Peach Bottom Unit 2 30° Capsule Packet G1 Fe Dosimeter Wire G1 Fe: Prior to Cleaning (left); and After Cleaning/Coiling (right)**

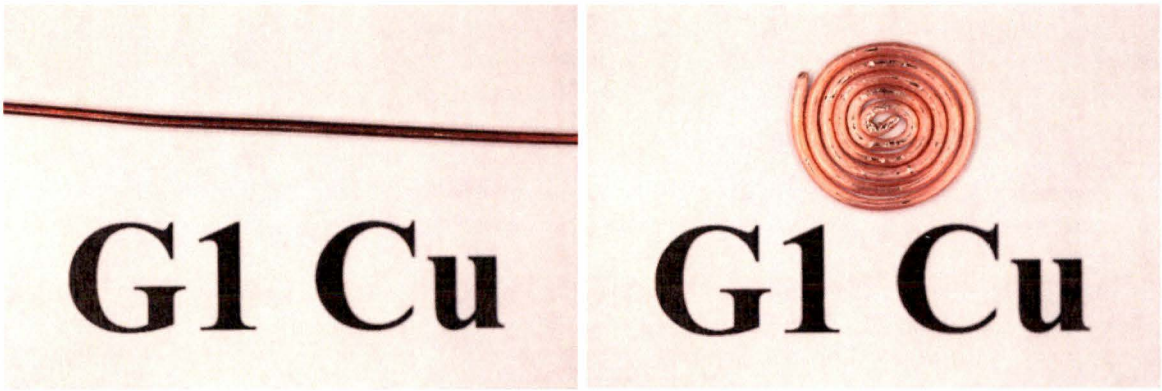


**Figure A-2**
**Peach Bottom Unit 2 30° Capsule Packet G1 Cu Dosimeter Wire G1 Cu: Prior to Cleaning (left); and After Cleaning/Coiling (right)**

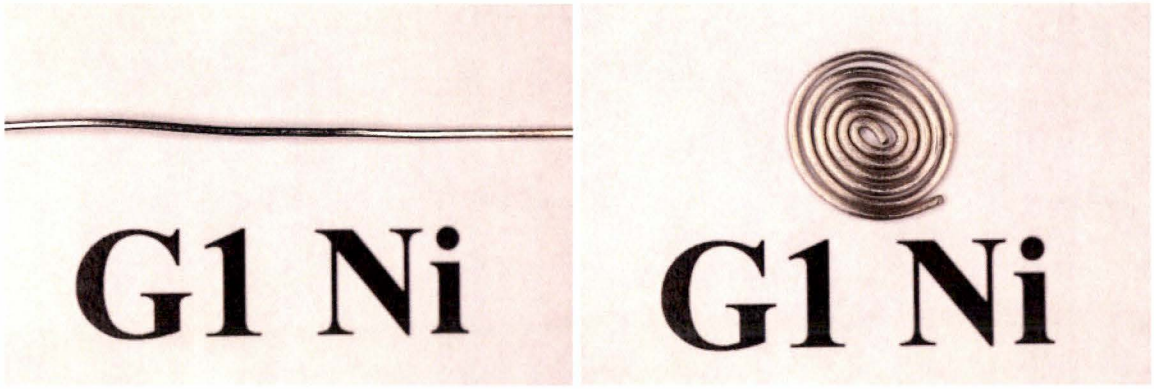


**Figure A-3**
**Peach Bottom Unit 2 30° Capsule Packet G1 Ni Dosimeter Wire G1 Ni: Prior to Cleaning (left); and After Cleaning/Coiling (right)**

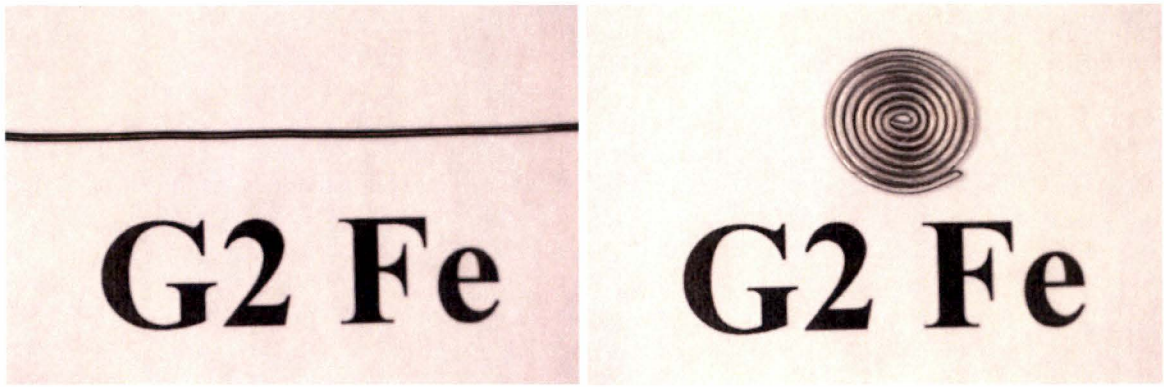


**Figure A-4**
**Peach Bottom Unit 2 30° Capsule Packet G2 Fe Dosimeter Wire G2 Fe: Prior to Cleaning (left); and After Cleaning/Coiling (right)**

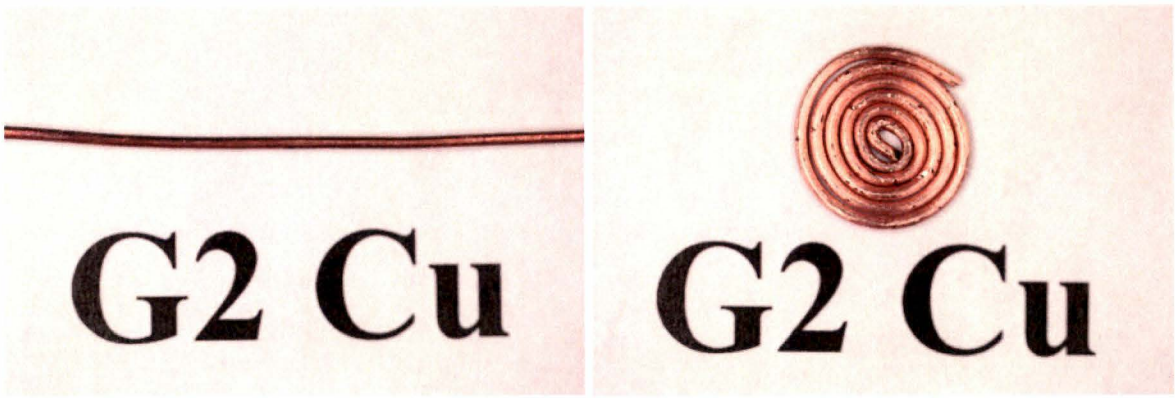


**Figure A-5**
**Peach Bottom Unit 2 30° Capsule Packet G2 Cu Dosimeter Wire G2 Cu: Prior to Cleaning (left); and After Cleaning/Coiling (right)**

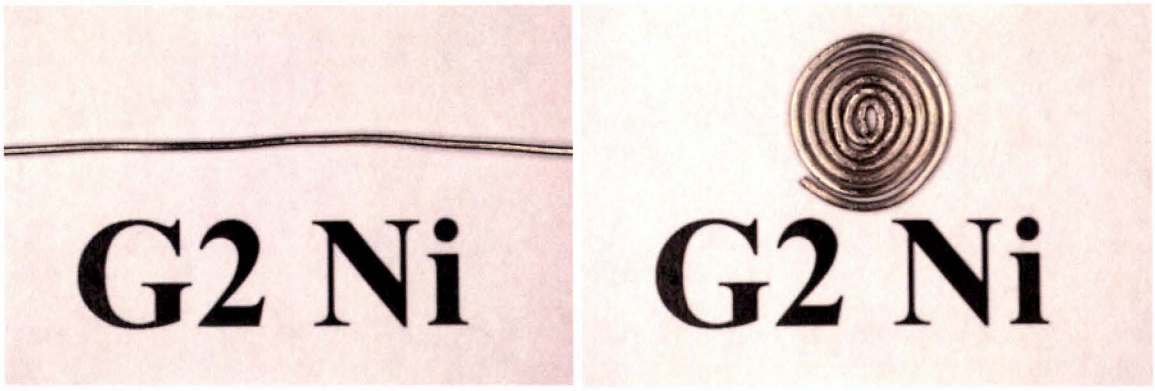


**Figure A-6**
**Peach Bottom Unit 2 30° Capsule Packet G2 Ni Dosimeter Wire G2 Ni: Prior to Cleaning (left); and After Cleaning/Coiling (right)**

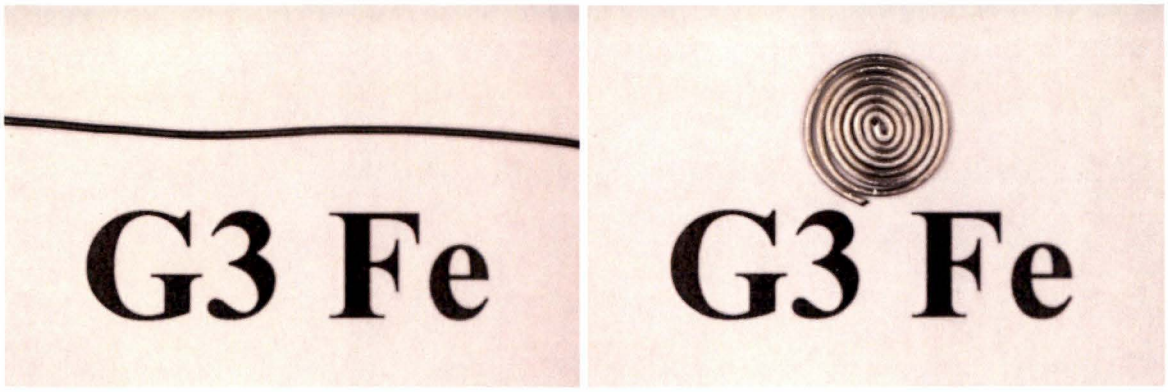


**Figure A-7**
**Peach Bottom Unit 2 30° Capsule Packet G3 Fe Dosimeter Wire G3 Fe: Prior to Cleaning (left); and After Cleaning/Coiling (right)**

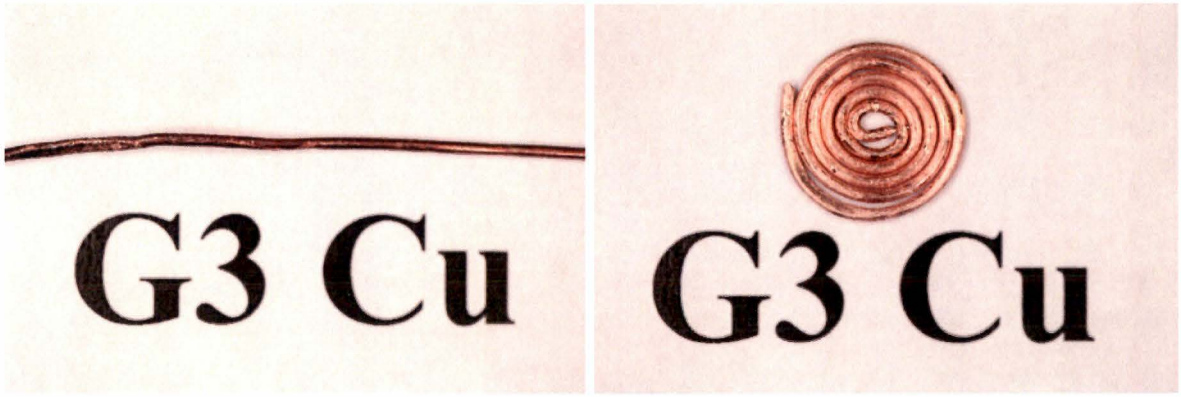


**Figure A-8**
**Peach Bottom Unit 2 30° Capsule Packet G3 Cu Dosimeter Wire G3 Cu: Prior to Cleaning (left); and After Cleaning/Coiling (right)**

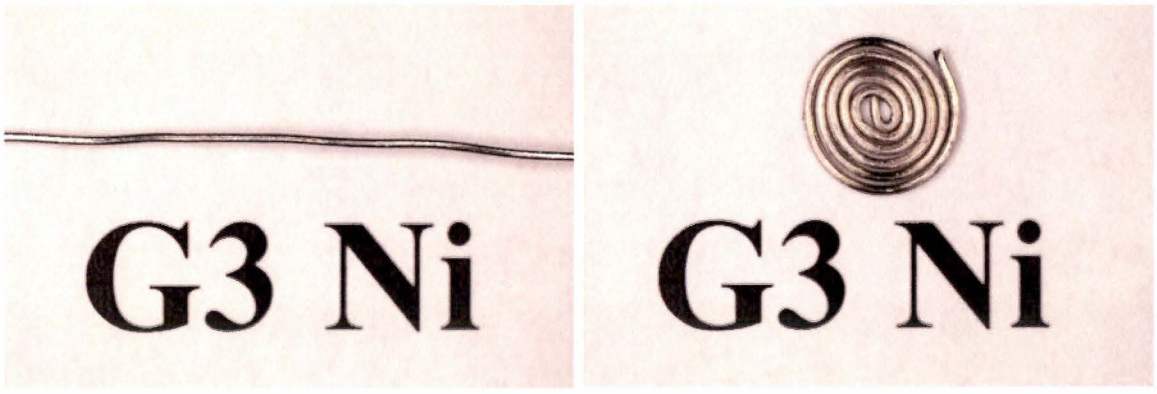


**Figure A-9**
**Peach Bottom Unit 2 30° Capsule Packet G3 Ni Dosimeter Wire G3 Ni: Prior to Cleaning (left); and After Cleaning/Coiling (right)**

**Table A-1**
**Peach Bottom Unit 2 30° Capsule Charpy Packet Dosimeter Wire Masses**

| Wire Dosimeter ID | Mass (mg) |
|---|---|
| G1 Fe | 162.73 |
| G1 Cu | 393.96 |
| G1 Ni | 281.68 |
| G2 Fe | 160.69 |
| G2 Cu | 403.97 |
| G2 Ni | 284.55 |
| G3 Fe | 160.09 |
| G3 Cu | 389.03 |
| G3 Ni | 261.18 |

**Table A-2**
**Gamma Ray Spectrometer System (GRSS) Specifications**

| System Component | Description and/or Specifications |
|---|---|
| Detector | Canberra Model BE3830 |
| Energy Resolution | <1.9 keV FWHM @ 1.33 MeV |
| Detector Efficiency Relative to a 3 inch x 3 inch NaI Crystal | 33.3% at 1.3 MeV |
| Amplifier/Multichannel Analyzer | Canberra DAS-1000 |
| Computer System | Intel i5-4460 CPU at 3.20 GHz, 16 GB Main Memory, 931 GB Hard Disk, 23-inch Monitor, HP LaserJet Printer |
| Software | Canberra Apex v 1.4 |

**Table A-3**
**Counting Schedule for Peach Bottom Unit 2 30° Capsule Dosimeter Materials**

| Dosimeter ID | Count Start Date | Count Start Time (EST) | Count Duration (Live Time Seconds) |
|---|---|---|---|
| G1 Fe | 12/4/2019 | 5:32:11 PM | 86,400 |
| G1 Cu | 11/21/2019 | 3:58:33 PM | 86,400 |
| G1 Ni | 11/24/2019 | 8:02:29 AM | 86,400 |
| G2 Fe | 12/3/2019 | 2:11:51 PM | 86,400 |
| G2 Cu | 11/20/2019 | 3:17:40 PM | 86,400 |
| G2 Ni | 11/25/2019 | 9:25:02 AM | 86,400 |
| G3 Fe | 12/2/2019 | 9:38:43 AM | 86,400 |
| G3 Cu | 11/22/2019 | 4:56:35 PM | 86,400 |
| G3 Ni | 11/26/2019 | 2:03:45 PM | 86,400 |

**Table A-4**
**Neutron-Induced Reactions of Interest**

| Dosimeter Material | Neutron-Induced Reaction | Reaction Product Radionuclide |
|---|---|---|
| Iron | $Fe^{54}(n,p)Mn^{54}$ | $Mn^{54}$ |
| Copper | $Cu^{63}(n,\alpha)Co^{60}$ | $Co^{60}$ |
| Nickel | $Ni^{58}(n,p)Co^{58}$ | $Co^{58}$ |

**Table A-5**
**Results of Peach Bottom Unit 2 30° Capsule Radiometric Analysis**

| Dosimeter ID | Isotope ID | Activity at Reference Date/Time[1] (μCi) | Specific Activity at Reference Date/Time[1] (dps/mg) | Activity Uncertainty (%) |
|---|---|---|---|---|
| G1 Fe | $^{54}Mn$ | 3.30E-01 | 75.03 | 2.21 |
| G1 Cu | $^{60}Co$ | 1.25E-01 | 11.74 | 1.70 |
| G1 Ni | $^{58}Co$ | 6.86E+00 | 901.09 | 2.29 |
| G2 Fe | $^{54}Mn$ | 3.25E-01 | 74.83 | 2.22 |
| G2 Cu | $^{60}Co$ | 1.23E-01 | 11.27 | 1.71 |
| G2 Ni | $^{58}Co$ | 6.93E+00 | 901.11 | 2.29 |
| G3 Fe | $^{54}Mn$ | 3.29E-01 | 76.04 | 2.21 |
| G3 Cu | $^{60}Co$ | 1.21E-01 | 11.51 | 1.70 |
| G3 Ni | $^{58}Co$ | 6.34E+00 | 898.15 | 2.29 |

[1] October 15, 2018 at 12:30:00 AM EST is the reference date and time.

**The Electric Power Research Institute, Inc.** (EPRI, www.epri.com) conducts research and development relating to the generation, delivery and use of electricity for the benefit of the public. An independent, nonprofit organization, EPRI brings together its scientists and engineers as well as experts from academia and industry to help address challenges in electricity, including reliability, efficiency, affordability, health, safety and the environment. EPRI also provides technology, policy and economic analyses to drive long-range research and development planning, and supports research in emerging technologies. EPRI members represent 90% of the electricity generated and delivered in the United States with international participation extending to nearly 40 countries. EPRI's principal offices and laboratories are located in Palo Alto, Calif.; Charlotte, N.C.; Knoxville, Tenn.; Dallas, Texas; Lenox, Mass.; and Washington, D.C.

Together...Shaping the Future of Electricity

***Program:***

Boiling Water Reactor Vessel and Internals Program (BWRVIP)



3002018177

**Electric Power Research Institute**
3420 Hillview Avenue, Palo Alto, California 94304-1338 • PO Box 10412, Palo Alto, California 94303-0813 USA
800.313.3774 • 650.855.2121 • askepri@epri.com • www.epri.com